Running head:

STRATIGRAPHIC ARCHITECTURE OF MIXED TIDE-AND-WAVE-INFLUENCED DELTA

Title:

FACIES RELATIONSHIPS AND STRATIGRAPHIC ARCHITECTURE OF DISTAL, MIXED TIDE-AND-WAVE-INFLUENCED DELTAIC DEPOSITS: LOWER SEGO SANDSTONE, WESTERN COLORADO, USA

Authors:

BERIT LEGLER[1,2], GARY J. HAMPSON*[1], CHRISTOPHER A-L. JACKSON[1], HOWARD D. JOHNSON[1], BENÔIT Y.G. MASSART[1,3], MARCUS SARGINSON[4,5] & RODMAR RAVNÅS[4]

[1]Department of Earth Science and Engineering, Imperial College London, South Kensington Campus, London SW7 2AZ, UK.

[2]present address: Wintershall Holding GmbH, Friedrich-Ebert-Strasse 160, 34119 Kassel, Germany.

[3]Statoil ASA, Sandsliveien 90, Postboks 7200, 5020 Bergen, Norway.

[4]Norske Shell, Tankvegen 1, 4056 Tananger, Norway.

[5]present address: Murphy Sarawak Oil Company Ltd., Petronas Twin Towers, 50088 Kuala Lumpur, Malaysia.

*E-mail address of corresponding author:

g.j.hampson@imperial.ac.uk

Key words:

tides, waves, delta, Sego Sandstone, Book Cliffs

ABSTRACT

The facies characteristics and stratigraphic architectures of ancient mixed, wave-and tide-influenced deltas are poorly documented, despite the abundance of analogous modern shorelines. This paper presents the first facies analysis and stratigraphic-architectural characterization of the distal part of the Cretaceous lower Sego Sandstone (Book Cliffs, Colorado, USA), whose correlative proximal part is arguably the most comprehensively documented example of ancient deltaic strata that exhibit evidence for the activity of tides and waves.

The distal lower Sego Sandstone consists of tide-dominated and wave-dominated deposits arranged within four regressive-transgressive tongues bounded by flooding surfaces. The proximal part of each regressive-transgressive tongue contains tide-dominated sandstones that sharply to erosionally overlie, and laterally interfinger with, wave-dominated deposits in the distal part of the tongue. Tide-dominated sandstones are fine to medium grained, and comprise wavy bedded and cross-bedded sandstones with abundant mud drapes, reactivation surfaces and bidirectional, ebb- and flood-tide-directed paleocurrents. They define active tidal distributary channel-fill and non-channelized tidal bar deposits of similar lithologic character, which represent the proximal part of the delta front. Abandoned tidal distributary channel fills comprise intensely bioturbated mudstones. The outer, paleoseaward parts of tidal bars contain direct evidence for mixed tide and wave influence in the form of hummocky cross-stratified, very fine-grained sandstone beds intercalated with cross-bedded, fine- to medium-grained sandstones containing tidal indicators. These deposits locally pass paleoseaward into low-angle and hummocky cross-stratified sandstones of similar grain size and texture to tidal bar deposits, implying reworking by storm waves. Wave-dominated deposits consist of coarsening-upward successions of mudstone and hummocky cross-stratified sandstone beds that represent the distal part of the delta front. Localized rhythmic variations in the wavelength of hummocky cross-stratification within some deposits may record tidal modulation of water depth and storm-wave velocities.

These facies components and their architectural arrangement suggest that tides and waves operated together throughout deposition of the “lower Sego Delta”, but that tide-dominated and wave-dominated deposits were spatially partitioned into the proximal and distal parts of each regressive-transgressive tongue. Thus, tides and waves were effective in transporting and reworking sediment in different water depth ranges and at different geographic locations. Mixed tide-and-wave-influenced deposits are generally preserved only at the down-dip pinchout of regressive-transgressive tongues,

because they are removed by tidal scour during delta progradation in more proximal locations. The spatial partitioning of time-equivalent tide-dominated and wave-dominated deposits is readily explained in a single depositional model, which requires the interpretation of neither sequence boundaries nor temporal changes in process regime across the sharp-to-erosional juxtaposition of tide-dominated sandstones above wave-dominated deposits in a regressive-transgressive tongue.
[end of abstract]

INTRODUCTION

Modern tide-influenced river deltas commonly display a complex interaction of waves and tides in their distal parts (e.g. Fly River Delta, Harris et al. 1993; Ganges-Brahmaputra Delta, Michels et al. 1998; Mekong Delta, Ta et al. 2005). Wave- and tide-dominated shorelines also co-exist laterally adjacent to each other in modern settings (e.g. Ainsworth et al. 2011). In contrast, the interaction of coeval tide and wave processes within the same depositional system has only rarely been documented in the rock record (e.g. wave-dominated, tide-influenced shoreface deposits; Dashtgard et al. 2012; Vakarelov et al. 2012). Typically, the dominance of waves and tides in ancient shallow-marine deposits is used as a criterion to differentiate different parts of a regressive-transgressive cycle, such that wave-dominated deposits are commonly assigned to regressive strata, and tide-dominated deposits to transgressive strata, including valley fills that underwent tidal amplification during transgressive drowning (e.g. Van Wagoner et al. 1990; Cross et al. 1993). More sophisticated approaches integrate the effects of basin paleogeography and bathymetry on shallow-marine process regime, but still tend to relate waves and tides to specific parts of a regressive-transgressive shoreline transit (e.g. Yoshida et al. 2007; Ainsworth et al. 2008). For example, tidal resonance of a bathymetrically compartmentalized basin may result in tide-dominated deposition during periods of falling and lowered relative sea level (e.g. Yoshida et al. 2007). The coeval interaction of waves and tides in an ancient river delta has only rarely been documented (e.g. Gani and Bhattacharya 2007).

The apparent scarcity of ancient deltas subject to significant mixed, wave and tide influence may reflect the grain-size dependence of bedforms generated by waves (e.g. hummocky cross-stratification in very fine- to fine-grained sand, and trough and planar cross-stratification in medium-grained sand; Yoshida et al. 2007), and the low preservation potential of wave-generated bedforms due to subsequent reworking by strong tidal currents (Pontén and Plink-Björklund 2009). The most obvious indication of wave influence in the distal parts of tide-influenced and tide-dominated deltaic successions is their diminished mud content relative to more proximal settings, resulting in

deposition of "clean" sandstones at the delta front (e.g. Eocene Roda Sandstone, Spain, López-Blanco et al. 2003; Dalrymple and Choi 2007). Ancient deltaic deposits that exhibit some degree of tide and wave influence are preferentially interpreted as tide-dominated (e.g. Eocene Misoa Formation, Venezuela, Maguregui and Tyler 1991; Cretaceous Haystack Mountain Formation, Wyoming, USA, Mellere and Steel 1995; Cretaceous Twentymile Sandstone, Colorado, USA, Seidler and Steel 2001; Devonian Kernave and Aruküla Formations, Baltic region, Tänavsuu-Milkeviciene and Plink-Björklund 2009) or as mixed, fluvial-and-tide-influenced systems (e.g. Cretaceous Frewens Sandstone, Wyoming, USA, Willis et al., 1999; Devonian Gauja Formation, Baltic region, Pontén and Plink-Björklund 2007).

This paper focusses on the facies characteristics and stratigraphic architecture of distal deltaic deposits in the lower part of the Cretaceous Sego Sandstone in the Book Cliffs, western Colorado, USA. Despite much previous work on the Sego Sandstone in the Book Cliffs (e.g. Van Wagoner 1991; Yoshida et al. 1996; Willis 2000; McLaurin and Steel 2000; Willis and Gabel 2001, 2003; Wood 2004; Aschoff and Steel 2011a), these distal deposits have not been studied in detail before. The aims of the paper are threefold: (1) to document the stratigraphic relationships between wave- and tide-dominated deposits in the distal lower Sego Sandstone; (2) to construct a depositional model that accommodates these stratigraphic relationships; and (3) to discuss the spatial and temporal relationships between waves and tides, and their implications for the interpretation of the lower Sego Sandstone as the deposits of a mixed, tide-and-wave-influenced delta.

GEOLOGIC SETTING

The Sego Sandstone is Middle Campanian, and occurs within the Mesaverde Group (Fouch et al. 1983). The unit is exposed in the Book Cliffs in eastern Utah and western Colorado (Fig. 1B). Previous studies have documented abundant evidence for tidal deposition within the Sego Sandstone (e.g. Van Wagoner 1991; Willis 2000; McLaurin and Steel 2000; Willis and Gabel 2001, 2003; Wood 2004). Towards the northwest (paleolandward; Fig. 1B-C), the Sego Sandstone passes either conformably (McLaurin and Steel 2000; Aschoff and Steel 2011a, 2011b) or unconformably (Yoshida et al. 1996; Willis 2000) into fluvial deposits of the Castlegate Sandstone. Towards the southeast (paleoseaward; Fig. 1B-C), the Sego Sandstone thins and passes into the offshore shales of the Mancos Shale (Kirschbaum and Hettinger 2004). The Sego Sandstone overlies the Buck Tongue of the Mancos Shale, and is overlain by coastal plain deposits of the Neslen Formation in eastern Utah and their shallow-marine correlatives in the Mount Garfield Formation in western Colorado (Fig. 1B-C) (Fisher 1936;

Fisher et al. 1960; Franczyk 1989; Franczyk et al. 1990; Hettinger and Kirschbaum 2002; Kirschbaum and Hettinger 2004). Marine shales of the Anchor Mine Tongue of the Mancos Shale subdivide the Sego Sandstone into lower and upper parts (Fig. 1C) (Erdmann 1934; Fisher 1936; Fisher et al. 1960).

Both the lower and upper parts of the Sego Sandstone form parts of a wedge of non-marine to shallow-marine siliciclastic sediment that thins and interfingers eastwards with open-marine mudstones of the Mancos Shale (e.g. Young 1955). This and other siliciclastic-sediment wedges in the Mesaverde Group were deposited along the western margin of the north-south-trending Cretaceous Western Interior Seaway (WIS) (Fig. 1A), which infilled a broad basin formed by a combination of relatively short-wavelength subsidence due to thrust-sheet loading in the Sevier Orogen at its western margin (e.g. Kauffman and Caldwell 1993) and long-wavelength subsidence driven by dynamic topography above the shallowly subducted Farallon plate (e.g. Liu et al. 2011, 2014). Sediment supply to the western margin of the seaway determined the location and timing of deposition of siliciclastic-sediment wedges, and was controlled by thrust-sheet emplacement and associated sediment routing in the Sevier Orogen (Krystinik and DeJarnett 1995). During deposition of the siliciclastic-sediment wedge containing the Sego Sandstone, thin-skinned thrust tectonics of the Sevier Orogeny may have transitioned to thick-skinned, basement-involved, tectonics of the Laramide Orogeny, giving rise to reduced subsidence and more pronounced progradation (Aschoff and Steel 2011a, 2011b).

Shoreline and nearshore deposits of the Mesaverde Group are generally wave- and storm-dominated (e.g. McGookey et al. 1972). Coriolis-driven circulation of surface waters (Parrish et al. 1984; Slingerland and Keen 1999) and storm-driven currents (Ericksen and Slingerland 1990; Slingerland and Keen 1999) both resulted in the development of a basinwide, counter-clockwise gyre in the WIS, which produced wave-driven, southward-directed, alongshore transport of sediment in nearshore settings. Tidal influence in the WIS is generally regarded as subordinate, and a micro-tidal regime is inferred for all paleoshorelines outside of the southeastern margin of the seaway (Ericksen and Slingerland 1990). However, various shallow-marine sandstones that are either isolated from, or were deposited within southward-deflected protrusions from, the north-south-trending regional paleoshorelines along the western margin of the seaway record strong local tidal processes (e.g. Mellere and Steel 1995, 2000; Nummedal and Riley 1999; Hampson et al. 2008). The apparently increased influence of tides during deposition of these sandstones is attributed to localized amplification of tidal currents passing through narrow, shallow straits and embayments, which formed via the subtle growth of tectonic structures on the sea floor, and whose effects were more pronounced during periods of lowered relative sea level (Martinsen 2003; Yoshida et al. 2007). Eastern

Utah and western Colorado lay within a broad embayment in the western paleoshoreline of the WIS (labelled "Utah Bight" in Fig. 1A; Zapp and Cobban 1960; McGookey et al. 1972), which underwent anomalously slow and spatially uniform subsidence during deposition of the Sego Sandstone (Aschoff and Steel 2011a, 2011b). Some workers have argued that as a result the Sego Sandstone built out across a broad region of irregular, shallow bathymetry that favored the enhancement of tides and suppression of waves (Steel et al. 2012); however, the regional correlation that underpins this interpretation is open to question (e.g. see alternative regional correlation in Hettinger and Kirschbaum 2002), and the inferred causal link between spatial subsidence patterns and enhanced tidal influence has yet to be quantitatively tested. During the middle Campanian, the study area occupied a subtropical paleolatitude (approximately 42°N) and had a warm, humid climate (Kauffman and Caldwell 1993).

Previous sedimentologic and sequence stratigraphic work on the lower Sego Sandstone

Two different sedimentologic and sequence stratigraphic interpretations have been developed previously for the lower Sego Sandstone in the Book Cliffs. The first interpretation, originally proposed by Van Wagoner (1991) and later modified by Willis (2000) and McLaurin and Steel (2000), assigns tidal sandstones to tidal bar deposits within a series of broad (<25 km), shallow (<20 m), vertically stacked incised valleys. The basal erosion surfaces of tidal sandstones are thus interpreted as sequence boundaries, which record valley incision into wave-dominated lower shoreface and offshore deposits during relative falls of sea level. Up to six incised valley fills (Van Wagoner 1991) are interpreted in the lower Sego Sandstone. This first interpretation implies that tidal amplification was restricted to estuaries that backfilled valleys during transgression.

The second interpretation was proposed by Willis and Gabel (2001), and then further developed by Willis and Gabel (2003), Wood (2004), Aschoff and Steel (2011a, 2011b), Burton and Wood (2011), and Steel et al. (2012). In this interpretation, tidal sandstones in the lower Sego Sandstone are assigned to the deposits of tidal bars located both inside and outside distributary channels, as part of tide-dominated deltas that were deposited in vertically stacked, regressive-transgressive shoreline tongues. The basal erosion surfaces of tidal sandstones were formed by tidal scour in front and at the base of tidal bars and fluvio-tidal distributaries (Willis and Gabel 2003). The lower, unbioturbated parts of the tidal sandstones record delta progradation, whereas the upper, bioturbated parts of the tidal sandstones record sediment starvation during the early phases of transgression. Each regressive-transgressive tongue is capped by a flooding surface. Three regressive-transgressive tongues are

198 generally interpreted in the lower Sego Sandstone (e.g. Willis and Gabel 2001). This second
199 interpretation invokes tidal resonance in the "Utah Bight" (Fig. 1A) during both regression and
200 transgression.
201
202 Both interpretations are based on data that show clear stratigraphic and/or areal partitioning of wave-
203 and tide-dominated deposits, and by extension infer temporal and/or spatial partitioning of wave and
204 tide processes. Wave-dominated deposition is either limited to regressive, highstand systems tracts
205 beneath incised valleys (e.g. Van Wagoner 1991) or to regressive, highstand-through-lowstand
206 systems tracts in the outer, distal parts of tide-dominated deltas (e.g. Willis and Gabel 2001). Both
207 interpretations are focussed on the proximal, axial parts of the Sego Sandstone depositional system, as
208 exposed in the central Book Cliffs (Fig. 1B), where tides were dominant. Broadly coeval deposits of
209 the Sego Sandstone exposed some 100 km north of the eastern Book Cliffs contain evidence of mixed
210 wave and tide processes, in the form of preserved remnants of barrier island systems (York et al. 2011;
211 Painter et al. 2013).
212
213 **DATASET AND METHODS**
214
215 The outcrop dataset presented here is taken from a c. 12 km-long, west-east-oriented stretch of the
216 Book Cliffs in western Colorado, between Jim Canyon in the west and Dry Canyon in the east (Fig. 2).
217 The cliffs provide near-continuous lateral exposure, and are dissected by numerous canyons that
218 provide a degree of three-dimensional control on facies relationships, sediment-body geometries, and
219 stratigraphic architectures. The cliff and canyon exposures represent c. 9 km along regional
220 depositional strike (from southwest to northeast) and c. 7 km down regional depositional dip (from
221 northwest to southeast) (Fig. 1B; Willis and Gabel 2001). Detailed measured sections, continuous
222 photomosaics along the cliff faces, and paleocurrent measurements were collected.
223
224 **FACIES ANALYSIS**
225
226 Facies schemes for the lower Sego Sandstone in the outcrops immediately to the west of the study
227 area were established previously by Van Wagoner (1991) and Willis and Gabel (2001). In this section,
228 we describe and interpret eight facies associations in the Buck Tongue and lower Sego Sandstone in
229 the study area, by expanding on these existing facies schemes. Facies analysis is based on
230 observations of lithology, grain size and sorting, sedimentary structures, paleocurrents, body fossils,

and trace fossils. Facies associations are illustrated with outcrop photographs (Figs. 3, 4, 5), representative measured sections (Fig. 6), and summary measured sections (Fig. 7).

Facies Association 1: Coarsening-upward successions of mudstone and hummocky cross-stratified sandstones

Description.--- FA1 characterizes the Buck Tongue Member. Claystones, siltstones, and very fine-grained sandstones are arranged into coarsening-upward successions that are 1-12 m thick and 100s-1000s m in lateral extent (e.g. 0-5 m in Fig. 6A, 0-4 m in Fig. 6B, 0-10 m in Fig. 6C). Claystones and siltstones are usually structureless or laminated, and lenses and wavy beds of fine-grained sandstones are intercalated (Fig. 3A). Bioturbation is generally sparse to moderate, but is intense in some beds. Very fine-grained sandstones form beds up to a few 10s cm thick that contain hummocky cross-stratification (HCS), low-angle cross-lamination, and rare swaley cross-stratification (SCS). The sandstone beds are sparsely bioturbated by *Ophiomorpha* at their tops.

Interpretation.--- Claystone- and siltstone-dominated deposits of FA1 represent deposition principally below storm wave base. Sandstone beds containing HCS, SCS, and bioturbated tops are interpreted to record deposition by strong oscillatory or combined flows during storm events (e.g. Duke 1985; Dumas et al. 2005). The upwards increase in thickness and abundance of these sandstone beds is interpreted to represent an upward shallowing of water depth, an upward increase in the energy of the prevailing storm-wave climate, and/or increased sand supply (e.g. Dott and Bourgeois 1982; Storms and Hampson 2005). Mudstones intercalated between storm-event sandstone beds represent fair-weather deposition, potentially in combination with fine-grained storm event beds (e.g. wave-supported gravity flows or fluid-mud flows; Kineke et al. 1996; MacQuaker et al. 2010). The variable intensity of bioturbation in the mudstones implies variable sedimentation rates and/or salinity conditions consistent with an overall deltaic setting (MacEachern and Bann 2008). FA1 is interpreted to represent deposition in a distal lower shoreface or inner shelf environment (see also Van Wagoner, 1991 and Willis and Gabel, 2001).

Facies Association 2: Hummocky cross-stratified sandstones

Description.--- FA2 occurs in the Buck Tongue Member and gradationally overlies FA1, to form the upper, sandstone-dominated parts of coarsening-upward successions. Very fine-grained sandstone beds containing HCS, SCS, and low-angle cross-lamination are amalgamated to form units that are

several meters thick (Fig. 3B; e.g. 5-12 m in Fig. 6A). Amalgamated sandstone beds commonly have large (up to 0.5 m deep) gutter casts at their bases (Fig. 6), and are sparsely bioturbated by *Ophiomorpha*. Thin (<0.2 m) intercalations of claystone and siltstone, which contain centimeter-thick beds of very fine-grained sandstone, occur locally, and are structureless or wavy bedded and moderately to intensely bioturbated. Units of FA2 can be traced laterally for 100s-1000s m and thin towards the southeast.

Interpretation.--- Amalgamated sandstone beds containing HCS and SCS were deposited above storm wave base (e.g. Dott and Bourgeois 1982; Duke 1985). Gutter casts at the base of these beds formed by erosion of the seabed by storm-generated eddies (cf. Whitaker 1973). Local mudstone intercalations represent fair-weather deposition. Units of FA2 in the upper parts of upward-coarsening successions that contain FA1 in their lower parts are interpreted to record a continued shallowing, continued increase in energy of storm-wave climate and/or continued increase of sand supply. FA2 is interpreted to have been deposited in a proximal lower shoreface environment (Van Wagoner 1991; Willis and Gabel 2001). Southeastward thinning of FA2 is consistent with increasing water depth and distance from a sandy shoreline down regional depositional dip.

Facies Association 3: Interbedded hummocky cross-stratified and wave-rippled sandstones

Description.--- FA3 occurs locally in the uppermost part of the Buck Tongue Member and is directly overlain by the lower Sego Sandstone. The facies association contains amalgamated beds of very fine-grained sandstone that are 0.2-0.5 m thick and contain HCS of different scales that are intercalated in a quasi-rhythmic pattern. Typical HCS with a hummock-to-hummock wavelength of 1-2 m passes vertically into "micro HCS" of 10-20 cm wavelength and wave-ripple cross-lamination (Fig. 3C-E). In some instances, centimeter-thick mudstones are also rhythmically intercalated. Sandstones are sparsely bioturbated by *Ophiomorpha* at bed tops. Units of FA3 are several meters thick (e.g. 12-15 m in Fig. 6B) and 100s m in lateral extent.

Interpretation.--- Although similar in many respects to proximal lower shoreface deposits of FA2, the quasi-rhythmic stacking and superposition of storm-wave-generated structures at different scales in FA3 implies a different depositional environment. These quasi-rhythmically superimposed structures may represent amalgamated storm-event beds, each with preserved waning-flow deposits at its top, with intercalated mudstones deposited in fair-weather periods between storms. However, an alternative interpretation is offered by Yang et al. (2008). In wave-dominated shorefaces with

299 significant tidal influence, tidal fluctuation in water depth causes variation of storm-wave height and
300 intensity over each tidal cycle. During storms of longer duration than one tidal cycle, a rhythmic
301 variation in water depth and associated storm-wave wavelength produces tidally modulated storm
302 deposits. Based on the quasi-rhythmic variation in wavelength of storm-wave-generated structures,
303 the occurrence of rhythmical mudstone intercalations, and the general association with tidal deposits,
304 we interpret this facies association to record deposition in a tidally modulated, wave-dominated
305 shoreface environment. Similar deposits have not previously been described from the lower Sego
306 Sandstone.
307
308 ***Facies Association 4: Amalgamated low-angle cross-stratified sandstones***
309
310 **Description.---** FA4 occurs in the uppermost part of the Buck Tongue Member immediately below the
311 lower Sego Sandstone. FA4 is composed of fine-grained, low-angle cross-stratified and HCS-bearing
312 sandstones, which are coarser grained than FA2 and FA3, and are texturally similar to overlying and
313 laterally adjacent tidal deposits (FA5, FA6, FA7). Sandstones contain carbonaceous mud drapes and
314 hematite-cemented mud clasts (Figs. 3F-G), and are less well cemented than the sandstones of FA2
315 and FA3. Sandstones are sparsely bioturbated by *Ophiomorpha*. Units of FA4 are several meters thick
316 (e.g. 25-31 m in Fig. 6C) and laterally extensive over several kilometers, and increase in abundance
317 towards the southeast, down regional depositional dip.
318
319 **Interpretation.---** The occurrence of HCS indicates deposition of FA4 by storm waves (e.g. Duke 1985;
320 Dumas et al. 2005). The similar textural composition of sandstones in FA4 to overlying tidal
321 sandstones (FA6, FA7) and their occurrence gradationally down depositional dip of tidal sandstones
322 (FA5) imply that FA4 is genetically related to these tidal sandstones. We interpret FA4 as the distal
323 parts of tidal bars, represented by FA6 and FA7, that were completely reworked and redeposited by
324 storm waves. This interpretation is supported by the detailed stratigraphic relationships between FA4
325 and adjacent facies associations, as documented in a later section. The increased abundance of FA4
326 towards the southeast implies greater storm-wave reworking of tidal sandstones down regional
327 depositional dip.
328
329 ***Facies Association 5: Interbedded cross-bedded and hummocky cross-stratified sandstones***
330
331 **Description.---** FA5 occurs in the lower Sego Sandstone and is increasingly abundant in the
332 southeastern part of the study area. Very fine-grained sandstones, fine- to medium-grained

sandstones, and locally siltstones are intercalated to form units that are up to 8 m thick (e.g. 32-37 m and 38-42 m in Fig. 6C). Very fine-grained sandstone is planar laminated or contains HCS. Trough- and planar-cross bedding, wavy bedding, and low-angle cross-bedding are common in fine- to medium-grained sandstones. In the basal part of the lower Sego Sandstone, units of FA5 exhibit a cyclic stacking of fine- to medium-grained cross-bedded sandstone, very fine-grained HCS sandstone, and laminated siltstone (Fig. 4). Fine- to medium-grained, cross-bedded sandstones contain thin drapes of mud and carbonaceous material, and cross-beds locally contain mud pebbles. Elsewhere in the lower Sego Sandstone, mud drapes are exceptionally rare, bedding is often indistinct, and units of FA5 show either subtle fining-upward or coarsening-upward trends. Very fine-grained planar-laminated and HCS-bearing sandstones occur in intervals 0.1-2 m thick that are locally intensely bioturbated by *Ophiomorpha*. These bioturbated intervals are laterally continuous for kilometers and occur at the top of units of FA5. Measured paleocurrent directions in cross-bedded sandstones indicate dominant sediment transport towards the southeast, but paleocurrent directions towards the south-southwest and north-northwest are also common (Fig. 7). FA5 occurs in tabular units that are 100s-1000s m in lateral extent, gradationally pass into FA6 or FA7 to the northwest (up depositional dip), and interfinger with and transition into FA4 and FA2 to the southeast (down depositional dip). Typically, tabular units of FA5 gradationally overlie FA2, but may overlie FA6 across a sharp-to-erosional contact.

Interpretation.--- The occurrence of mud and carbonaceous drapes in cross-beds, and of bidirectional paleocurrents, in medium-grained sandstones implies deposition from tidal currents (as in FA6 and FA7) (e.g. Nio and Yang 1991), whereas the occurrence of HCS in very fine-grained sandstones indicates deposition from storm waves (as in FA1-4). The coexistence of both sets of structures in FA5 implies deposition by mixed tidal and storm-wave processes in an environment that was spatially transitional between proximal tide-dominated deposits (to the northwest) and distal wave-dominated deposits (to the southeast). We interpret cyclic interbedding of tide-dominated, medium-grained sandstones with mud drapes and storm-wave-dominated, very fine-grained sandstones in units of FA5 at the base of the Sego Sandstone to record the intermittent reworking by storm waves of tidal bars. The absence of mud drapes in units of FA5 developed at higher stratigraphic levels implies that mud was near-continuously resuspended by wave action. The occurrence of laterally extensive units of FA5 implies that storm-wave-reworking was particularly efficient at particular times, probably during drowning of parts of the "lower Sego Delta", and widespread bioturbated intervals of FA5 have previously been interpreted to mark flooding surfaces (Van Wagoner 1991; Willis and Gabel 2001). The dominant paleocurrent direction towards the southeast indicates sediment transport

mainly down regional depositional dip, indicating a dominance of ebb-directed tidal currents and/or fluvial currents. North-northwest-directed paleocurrents are interpreted to record flood-directed tidal currents, and paleocurrents directed towards the south-southwest may reflect the influence of alongshore currents (cf. Slingerland and Keen 1999).

Facies Association 6: Coarsening-upward successions of heterolithic, cross-bedded sandstones

Description.--- FA6 is the predominant facies association in the lower Sego Sandstone in the study area. Units of FA6 are 2-12 m thick and comprise upward-coarsening successions of fine- to medium-grained, trough and planar cross-bedded sandstones with abundant mud clasts and carbonaceous drapes along the lower parts of the foresets and toesets (e.g. 13-15 m and 35-43 m in Fig. 6A; Fig. 5A). Units are either gradationally based or overlie low relief erosive surfaces that are lined by discontinuous mud-clast-conglomerate lags (Fig. 5B). Fine-grained, wavy-bedded sandstone with mud drapes and mud clasts occur in the lower parts of the units, above the basal mud-clast lags (Fig. 5C). These heterolithic sandstones are sparsely to moderately bioturbated (e.g. *Planolites, Psilonichnus lutimuratus*). Planar-cross bedded sandstone is increasingly abundant in the middle of the units, and passes upwards into planar- and trough-cross bedded sandstone in the upper parts of the units (Fig. 5D). Cross-set thickness increases upwards from c. 0.1 m to 0.5 m, from the lower to upper parts of FA6, and in places smaller cross-sets are superimposed on larger cross-sets. Cross-bedded sandstones lack bioturbation. Paleocurrents are directed mainly towards the southeast, with subordinate paleocurrents directed towards the north-northwest, south-southwest, and northeast (Fig. 7). Cross-set boundaries are mostly horizontal, but some dip at 3-8° towards the southwest, oblique to the dominant paleocurrent direction. Units of FA6 are laterally extensive for 100s-1000s m, and pass towards the southeast (down depositional dip) into FA5.

Interpretation.--- The occurrence of an upward-coarsening trend in grain size, upward-thickening of cross-set thickness, and abundant mud drapes along foresets and toesets of trough and planar cross-beds implies deposition of FA6 by migration of subtidal bars, as previously interpreted by Willis and Gabel (2001). The upward transition from heterolithic, wavy-bedded sandstone to cross-bedded sandstone in each unit of FA6 reflects an overall upward increase in current energy, resulting from progradation of one bar. Mud-clast lags lining an erosion surface at the base of some units records tidal scour, and the low relief of the erosion surfaces indicates erosion in an unconfined setting. Paleocurrent data suggest that the dominant sediment transport was via ebb-directed tidal currents towards the southeast, with subordinate flood-directed tidal currents towards the north-northwest.

Paleocurrents towards the south-southwest and northeast may record sediment transport by local deflected ebb and flood tidal currents, or by alongshore currents (cf. Slingerland and Keen 1999). The occurrence of inclined cross-set boundaries oblique to the dominant paleocurrent direction implies oblique-lateral accretion of bars via superposition of migrating-dune deposits (cf. Houbolt 1968), rather than down-current bar accretion (e.g. Mutti et al. 1985). The lateral continuity of FA6 is consistent with previously reconstructed dimensions of tidal bars in the lower Sego Sandstone, with widths of 0.6-1.2 km and preserved thicknesses of up to 12 m (Willis and Gabel 2001; Wood 2004). Tidal-bar deposits of FA6 become thinner and narrower towards their down-dip pinchouts, implying an oval geometry in plan view. The overall dominance of tidal processes in FA6 reflects either deposition in an environment sheltered from storm waves, or intense tidal reworking that precluded preservation of storm-wave-generated structures.

Facies Association 7: Fining-upward, channelized sandstones

Description.--- FA7 cuts into and laterally replaces FA6 in the northwestern part of the study area. FA7 consists of fine- to medium grained sandstones that are confined within concave-upward erosional surfaces, and occurs in units that are 4-10 m thick, 10s-100s m wide and define channelized geometries (Fig. 5E). The basal erosional surfaces are commonly lined with plant material and *Teredolites*-bored logs. These channelized units typically exhibit a fining-upward grain size trend, and consist of trough and planar cross-sets that thin upwards into ripple cross-laminated and wavy-bedded sandstones with intercalated mudstones (e.g. 21-27 m in Fig. 6A, 16-27 m in Fig. 6B). Trough and planar cross-beds locally contain bidirectional paleocurrents towards the south-southwest and north-northeast (Fig. 7), and are stacked to form pronounced herringbone cross-bedding (Fig. 5F). Elsewhere, paleocurrents are directed towards the east-southeast (Fig. 7). Carbonaceous material is rare in cross-sets, but where present it occurs as either single or paired drapes along foresets and toesets. Planar bedding is locally intercalated between cross-sets of opposed paleocurrent directions. Cross-set boundaries and overlying heterolithic strata are commonly inclined at 3-10° in orientations perpendicular to paleocurrent directions. Cross-bedded sandstones are generally not bioturbated, but overlying heterolithic deposits are sparsely to moderately bioturbated by *Planolites*, *Psilonichnus lutimuratus* (Nesbitt and Campbell 2002) (Fig. 5G), and indistinct burrows.

Interpretation.--- Concave-upward erosional surfaces that bound units of FA7 represent channel bases. Hence, we interpret FA7 as channel-fill successions, in accordance with the previous interpretation of Willis and Gabel (2001). Plant material lining the channel bases represents a lag

deposit, and indicates erosion of a vegetated coastal plain adjacent to the channels. The fining-upward grain-size trend within each channelized unit reflects an upward decrease in current velocity as the channel was filled, although the abundance of sandstone indicates a high overall energy due to active filling. The occurrence of abundant bidirectional cross-bedding and rare mud drapes, some of which are paired, indicates deposition by tidal currents subject to flow reversal and slack-water periods (e.g. Nio and Yang 1991). The presence of herringbone cross-bedding implies that channels acted as conduits for both flood-tidal and ebb-tidal currents. Inclined cross-set boundaries perpendicular to the dominant paleocurrent direction record lateral accretion of the channel margin, which is typical of channel-filling bars (Dalrymple and Rhodes 1995). The generally low bioturbation intensity reflects environmentally stressed conditions due to salinity fluctuations and/or high sedimentation rates. *Teredolites*-bored wood is consistent with marine influence (Bromley et al. 1984), and *Psilonichnus lutimuratus* is typical of tidal environments, having been reported from tidal flats, tidal inlets, and intertidal, estuarine point bars (Nesbitt and Campbell 2002, 2006). Based on our interpretation of tide-dominated deposition, in conjunction with an inferred connection to a fluvial system from previous interpretations of the lower Sego Sandstone (Van Wagoner 1991; Willis 2000; McLaurin and Steel 2000; Willis and Gabel 2001, 2003; Wood 2004; Aschoff and Steel 2011a), we interpret FA7 as the active fill deposits of fluvio-tidal distributary channels. The predominance of FA7 in the proximal, northwestern part of the study area, relative to the non-channelized tidal-bar deposits of FA6, supports a transition down depositional dip from confined channels on the lower delta plain to unconfined tidal bars on the delta front.

Facies Association 8: Intensely bioturbated, channelized mudstones

Description.--- FA8 is composed of channelized claystones, siltstones and fine-grained sandstones that occur above concave-upward erosion surfaces, which have up to 5 m of relief and are 10s m wide (Fig. 5H). Homogenous to indistinctly wavy bedded sandy claystones and siltstones are the dominant lithologies (Fig. 5I), but organic-rich mudstones and coals, which lack associated roots, are also present (Fig. 5J). Bioturbation is intense to complete, by a diverse assemblage of trace fossils including *Teichichnus*, *Planolites*, and *Chondrites*. The bases of units of FA8 are locally slightly gradational, due to bioturbation of the underlying strata. FA8 is most abundant in in the northwestern part of the study area, where it is associated with FA7, but occurs also in the southeastern part.

Interpretation.--- The fine-grained character of units of FA8 and the high intensity of bioturbation indicate low sedimentation rates in a channelized environment with stable salinities. The facies

association is interpreted to record the infilling of abandoned distributary channels, based on its association with active distributary channel fills (FA7). Coals at the top of some abandoned channel fills are interpreted to be allochthonous, because they lack underlying roots. Abandonment of distributary channels in modern tide-influenced deltas results in the interruption of sand input and the establishment of normal marine salinity within channels solely influenced by tides (Allen and Chambers 1998), which is consistent with the style of bioturbation observed in FA8. Abandoned channels have not been previously interpreted in the lower Sego Sandstone.

STRATIGRAPHIC ARCHITECTURE AND SEQUENCE STRATIGRAPHY

The lower Sego Sandstone shows an overall upward increase in sandstone content within the study area, consistent with overall progradation of the "lower Sego Delta" (Van Wagoner 1991; Willis and Gabel 2001). Six upward-coarsening units of wave-dominated shoreface deposits (WS1-6) interfinger with, and are overlain by, four southeastward-thinning wedges of tide-dominated sandstone (TS1-4). The thickness, extent, and internal facies-association trends of each stratigraphic unit are described below. Particular emphasis is placed on the down-dip transition of tide-dominated sandstones into mixed wave- and tide-influenced deposits, and their transition in turn into wave-dominated shoreface deposits. The architectural relationships are illustrated using correlation panels constrained by observations from the cliff faces (Fig. 8) and a more detailed bedding diagram along one large, particularly well-exposed cliff face (Fig. 9). Lateral relationships are presented in a series of facies-association distribution maps (Fig. 10). The stratigraphic units that we document in the study area are compared to the regional sequence stratigraphic frameworks established further west, up regional depositional dip (Van Wagoner 1991; Willis and Gabel 2001).

Wave-dominated units WS1 and WS2

Description.--- Lower shoreface deposits are largely restricted to the lower part of the studied interval. Two coarsening-upward packages of distal to proximal, wave-dominated lower shoreface deposits (FA1-2), assigned to units WS1 and WS2, are vertically stacked on top of each other below the level of the lowermost tidal sandstones in the study area (TS1) (Figs. 6, 8). The shoreface units are locally amalgamated along depositional strike (Fig. 8A), but are more clearly distinct as they thin towards the southeast of the study area, down depositional dip (Fig. 8B).

Interpretation.--- Amalgamation and splitting of wave-dominated shoreface units WS1 and WS2 may be attributed to variations in relative sea level, energy of the storm-wave climate, and sand supply (e.g. Storms and Hampson 2005). For example, interference of shore-normal tidal currents offshore of distributary-channel mouths with shore-parallel currents generated by oblique wave approach may have resulted in localized interruption of sand supply and lowered storm-wave energy. The top of unit WS1 cannot be traced up depositional dip to locations where it demonstrably corresponds to a landward dislocation of the shoreline, but instead unit WS1 appears to thin and shale out into the Buck Tongue Shale towards the southwest, along regional depositional strike (e.g. in Figure 3 of Van Wagoner 1991). The top surface of unit WS1 thus cannot be demonstrated to be a flooding surface, and is instead interpreted as a bedset boundary. In contrast, the top of unit WS2 is traced to the northwest, up depositional dip, to the top of tidal-sandstone unit TS1 (Fig. 8A). The potential origin of this surface is discussed below.

Tide-dominated unit TS1

Description.--- The lowermost unit of tidal sandstones is restricted to the westernmost part of the study area (TS1) (Figs. 6A, 8). These sandstones sharply overlie distal and proximal lower shoreface deposits (FA1, FA2) in various locations along depositional strike (sections 1 and 2 in Fig. 8A). Unit TS1 comprises tidal bar deposits (FA6) up to 6 m thick, and thins to zero as erosional scour into underlying wave-dominated, proximal lower shoreface deposits (FA2) decreases towards the north-northeast over a lateral distance of c. 3 km (Fig. 8A). The unit is also documented to thin to zero over a lateral distance of c. 3 km towards the southwest, along regional depositional strike, outside of the study area (labelled as tidal unit overlying "sequence boundary 1?" between sections 1 and 7 in Figure 3 of Van Wagoner 1991). Paleocurrents are northeast- to east-northeast-directed (Figs. 8A, 10B), perpendicular to the overall southeastward progradation direction of the "lower Sego Delta" (Van Wagoner 1991; Willis and Gabel 2001). The tidal bar sandstones are overlain by proximal lower shoreface deposits (FA2) of unit WS3, across a planar erosional surface (labelled FS100 in Figs. 6A, 8). Tide-dominated unit TS1 occurs at the same stratgraphic level as, and up depositional dip from, wave-dominated unit WS2 (Fig. 10B).

Interpretation.--- Unit TS1 is interpreted to record localized progradation of tidal bars, potentially lateral to or in front of major fluvio-tidal distributary channels. In the distal parts of tide-influenced and tide-dominated deltas, tidal bars form elongate, laterally discontinuous bodies (Willis 1995), which is consistent with the pinchouts of unit TS1 along regional depositional strike to define a 6-km-

wide sandstone body. In such unconfined settings, tidal bars typically migrate obliquely down depositional dip; paleocurrents oriented along regional depositional strike, as documented in unit TS1, may have resulted from local flow diversion at the downdip end of the bar (Stride et al. 1982). The juxtaposition of the proximal lower shoreface deposits of unit WS3 above the tidal bar deposits of unit TS1 is interpreted to record increased water depth, across a flooding surface associated with transgressive erosion by waves (FS100; Figs. 6A, 8). Such wave ravinement has been interpreted in association with flooding surfaces elsewhere in the Sego Sandstone, as a means to generate a flat, bevelled surface at the top of tidal bars (Willis & Gabel, 2001, 2003).

Comparison with regional stratigraphic framework.--- In locations to the west of the study area, Van Wagoner (1991) interpreted the sharp base and top of unit TS1 (his "tidal unit overlying sequence boundary 1?") as a sequence boundary at the base of an incised valley and a flooding surface, respectively. Unit TS1 is absent in the "Westwater study area" of Willis and Gabel (2001), which lies some 10 km west of our study area. Here the Buck Tongue contains multiple bedsets of hummocky cross-stratified, lower shoreface deposits (figure 3a in Willis and Gabel 2001) that correspond to units WS1-2, TS1, and WS3-4.

Wave-dominated units WS3 and WS4

Description.--- Two further coarsening-upward packages of distal to proximal lower shoreface deposits (FA1-4), assigned to units WS3 and WS4, are vertically stacked above tidal sandstone unit TS1. These two units underlie and/or are laterally adjacent to tidal sandstone unit TS2 (Figs. 6, 8, 10C). The shoreface units amalgamate and split with each other, and locally with underlying unit WS2, along depositional strike (Fig. 8A). WS3 and WS4 form distinct units towards the southeast of the study area, down depositional dip, where they are defined by clear upward-coarsening trends (between sections 10 and 11 in Fig. 8B). Also in this area, unit WS4 consists predominantly of wave-reworked tidal-bar deposits (FA4) that occur directly down depositional dip of, and interfinger updip with, the distal pinchout of tidal sandstone unit TS2 (between sections 8 and 10 in Figs. 8B, 10C; Fig. 4B-D).

Interpretation.--- Amalgamation and splitting of the sandstone beds comprising wave-dominated shoreface units WS3 and WS4 is attributed to variations in energy of the storm-wave climate and/or sand supply (e.g. Storms and Hampson 2005), in the absence of regional correlation that indicates a landward dislocation of the shoreline between them. The top of unit WS3 is thus interpreted as a

570 bedset boundary. The top of unit WS4 is traced to the northwest, up regional depositional dip, to the
571 top of tidal-sandstone unit TS2 Fig. 8B), and this surface is interpreted below.
572
573 ***Tide-dominated unit TS2***
574
575 **Description.---** Tidal sandstone unit TS2 can be traced across most of the study area, but thins to zero
576 towards the southeast (Figs. 8, 10C). The base of the unit is sharp and locally erosional, locally lined
577 by mudclast conglomerate, and exhibits up to 2 m of relief. Unit TS2 overlies proximal lower
578 shoreface deposits (FA2) of units WS3 and WS4, which are locally tidally modulated (FA3; 1 km
579 northwest of section 6 in Fig. 8A). In the western part of the study area, unit TS2 is up to 14 m thick
580 and contains active and abandoned channel-fill deposits (FA7, FA8) developed at two distinct
581 stratigraphic levels (between sections 1 and 2 in Fig. 8A). Channel fills are 0.4–1 km wide and up to 7
582 m deep. Tidal bars (FA6) dominate in the central part of the study area (between sections 3 and 8 in
583 Fig. 8). Both tidal-bar and active channel-fill deposits (FA6, FA7) are similar in facies character, and
584 are discriminated by the presence or absence of concave-upward, channelized erosional surfaces, a
585 distinction which proves difficult to apply in cliff-face exposures oriented parallel to local channel
586 axes. Paleocurrents within unit TS2 are bidirectional, and are approximately north- and south-
587 directed (Figs. 8, 10C). Tidal-bar deposits (FA6) pass southeastwards, down regional depositional dip,
588 into wave-influenced tidal-bar deposits (FA5) that thin and interfinger further to the southeast into
589 wave-reworked tidal-bar deposits (FA4) (between sections 8 and 10 in Fig. 8B, 10C; Fig. 4B-D). Unit
590 TS2 is overlain by a thin (<1 m), laterally extensive (c. 5 km) interval of distal lower shoreface deposits
591 (FA1) in the western part of the study area (assigned to unit WS5 in Figs. 6A; between sections 1 and 3
592 in Fig. 8A). This correlates eastwards (between sections 4 and 8 in Fig. 8) with an intensely
593 *Ophiomorpha*-burrowed surface capping a tidal-bar succession (FA6). In the southeastern part of the
594 study area, this surface is overlain by proximal lower shoreface deposits (FA2) (assigned to unit WS5
595 in Figs. 6B; between sections 9 and 11 in Fig. 8B).
596
597 **Interpretation.---** Unit TS2 is interpreted to record the seaward advance of a fluvio-tidal distributary
598 channel belt (between sections 1 and 2 in Fig. 8A) and associated tidal bars that occur in between the
599 distributary channels (between sections 3 and 8 in Fig. 8), which pass paleoseaward into wave-
600 influenced and wave-reworked tidal bars that were not confined by distributary channels (between
601 sections 9 and 11 in Fig. 8B) (Fig. 10C). This dip-oriented transition in facies associations demonstrates
602 the prevailing mixed influence of waves and tides on deposition. Paleocurrent directions in tidal bars
603 and fluvio-tidal distributary channels indicate ebb- and flood-directed currents, oriented locally

towards the south and north (Figs. 8, 10C). The spread in paleocurrent directions likely reflects local variations in paleoflow around tidal bars and through channels. The distal parts of tidal bars were episodically eroded and reworked by storm waves, resulting in bed-scale interfingering of wave-influenced and wave-reworked tidal-bar deposits (FA4, FA5) (Fig. 4B-D). The resulting sediment redistribution probably reduced the height of the bars and increased their lateral extents along local depositional dip and strike. The local occurrence of tidally modulated proximal lower shoreface deposits in underlying units WS3 and WS4 implies that the latter are genetically related to unit TS2, and that the sharp-to-erosional base of unit TS2 reflects locally varying submarine tidal scour, as envisaged in the interpretations of Willis and Gabel (2001, 2003). The relatively low relief (<2 m) of the base of unit TS2 in the study area contrasts with the deep erosional relief documented in more westerly outcrops of this unit, up regional depositional dip (up to 15 m; Van Wagoner 1991; Willis and Gabel 2001, 2003). We attribute the differences in erosional relief to the action of confined tidal currents with higher peak velocity in a proximal deltaic setting, resulting in deeper scour, and weakly confined tidal currents in a distal deltaic setting (Willis and Gabel 2001; Willis 2005). The top of unit TS2 is interpreted to record an increase in water depth, from tidal-bar and channel-fill deposits in unit TS2 to overlying proximal lower shoreface deposits of unit WS5, across a flooding surface (FS200; Figs. 6, 8). The near-planar geometry of the flooding surface may reflect bevelling of the tops of tidal bars by wave ravinement (Willis & Gabel, 2001, 2003).

Comparison with regional stratigraphic framework.--- Unit TS2 corresponds to the "tidal units overlying sequence boundaries 3 and 4" of Van Wagoner (1991), as interpreted at the western margin of the study area, and by implication to "sandstone 1" of Willis and Gabel (2001) in their "Westwater study area". Van Wagoner (1991) interpreted the sharp-to-erosional base of unit TS2 as a sequence boundary at the base of an incised valley (his "sequence boundary 3"), whereas scour at this surface was instead attributed to submarine "lowstand tidal erosion" by Willis and Gabel (2001). The genetic linkage interpreted above of tide-dominated deposits in unit TS2 with wave-dominated deposits in units WS3 and WS4 supports the interpretation of coeval wave and tide activity (Willis & Gabel 2001), rather than a valley-fill interpretation in which waves were dominant during regression and tides during transgression (Van Wagoner 1991; Yoshida et al. 1996; Willis 2000). Vertical stacking of two distributary channel belts within unit TS2 (between sections 1 and 2 in Fig. 8A) is reflected in the interpretation by Van Wagoner (1991) of a second valley-bounding sequence boundary at the base of the upper distributary channel belt (his "sequence boundary 4"), but this surface cannot be traced further eastward in tidal-bar and channel-fill deposits in the study area (between sections 3 and 9 in

637 Figs. 8, 9). The top of unit TS2 has been previously interpreted as a flooding surface in outcrops to the
638 west of the study area (Van Wagoner 1991; Willis and Gabel 2001).
639
640 ***Wave-dominated unit WS5***
641
642 **Description.---** Unit WS5 consists of a thin (<1 m), laterally extensive (c. 5 km) interval of distal lower
643 shoreface deposits (FA1) in the western part of the study area (Fig. 6A; between sections 1 and 3 in
644 Fig. 8A), an intensely bioturbated surface capping a tidal-bar succession (FA6) in the central part of
645 the study area (between sections 4 and 8 in Fig. 8), and an eastward-thickening wedge of wave-
646 dominated proximal lower shoreface deposits (FA2) in the eastern part of the study area (Fig. 6C;
647 between sections 9 and 11 in Fig. 8B). In the western and central parts of the study area, unit WS5 is
648 sharply overlain by tidal-bar deposits (FA6; assigned to unit TS3 in Fig. 8). In the eastern part of the
649 study area, unit WS5 interfingers with wave-influenced tidal bar deposits (FA5; Fig. 8B). These
650 stratigraphic relationships with unit TS3 are interpreted below.
651
652 ***Tide-dominated unit TS3***
653
654 **Description.---** Tidal-sandstone unit TS3 extends throughout the study area, and at different locations
655 either: (1) coarsens upward gradationally from wave-dominated distal lower shoreface deposits (FA1)
656 of unit WS5 (sections 1-3 in Figs. 6A, 8A); (2) sharply overlies a surface marked by intense
657 bioturbation by *Ophiomorpha* (sections 4-8 in Fig. 8); (3) or sharply overlies wave-dominated proximal
658 lower shoreface deposits (FA2) of unit WS5 (sections 10-11 in Figs. 6C, 8B). The unit is up to 9 m thick,
659 and is dominated by tidal-bar deposits (FA6) with a small proportion of associated active channel-fill
660 deposits (FA7) (between sections 1 and 8 in Fig. 8). Towards the southeast, down regional
661 depositional dip, tidal-bar deposits (FA6) pass into wave-influenced tidal-bar deposits (FA5)
662 (between sections 8 and 9 in Figs. 8B, 10D) that extend to the southeastern limit of the study area.
663 Paleocurrent directions are bidirectional, and are locally oriented towards the north and south or
664 towards the northwest and southeast (Figs. 8, 10D). Unit TS3 is overlain by wave-dominated distal
665 lower shoreface deposits (FA1) that are up to c. 2 km in lateral extent (sections 7 and 10 in Fig. 8),
666 assigned to unit WS6, or by a laterally correlative, intensely *Ophiomorpha*-burrowed surface (sections
667 1-5, 8, 9, and 11 in Fig. 8).
668
669 **Interpretation.---** Unit TS3 contains a similar westward-to-eastward trend in facies associations, from
670 fluvio-tidal distributary channel-fill and tidal-bar deposits in the west to wave-influenced tidal-bar

deposits in the east, as that documented in unit TS2, and a similar interpretation is applied to both units. Progradation of tide-dominated unit TS3 is thus inferred to have been time-equivalent and genetically linked to that of the wave-dominated unit WS5 (Fig. 10D; cf. Willis & Gabel 2001), rather than to have occurred during later filling of a valley (cf. Van Wagoner 1991; Yoshida et al. 1996; Willis 2000), and the locally sharp base of TS3 is attributed to submarine tidal scour during progradation. Relative to units TS2 and WS4, facies-association belts in units TS3 and WS5 extend further eastward (Figs. 8, 10C-D), indicating overall basinward advance of the "lower Sego Delta". Distributary channels in the proximal part of the unit (between sections 1 and 2 in Figs. 8A, 10D) occur in comparable locations to those in unit TS2, implying a relatively stable position of the channel belts, and a possible upstream control on their position. Lateral variations in the character of the base of unit TS3 reflects variability in the location and depth of tidal scour at the base of the component tidal-bar deposits of unit TS3, with the central parts of the bar being erosionally based and their distal parts being gradationally based (Burton and Wood 2011). Paleocurrent directions are interpreted to reflect ebb- and flood-tidal currents roughly perpendicular to the shoreline, with local variability in shoreline orientation accounting for the spread in paleocurrent data. The top of unit TS3 is interpreted to record an increase in water depth across a flooding surface (FS300; Figs. 6, 8), from tidal-bar and channel-fill deposits in unit TS2 to overlying distal lower shoreface deposits of unit WS6. Wave ravinement may have sculpted the near-planar geometry of the flooding surface (Willis & Gabel, 2001, 2003).

Comparison with regional stratigraphic framework.--- Unit TS3 is contiguous with the lower part of the "tidal unit overlying sequence boundary 5" of Van Wagoner (1991) to the west of the study area, and to the lower part of "sandstone 2" of Willis and Gabel (2001) in their "Westwater study area". Van Wagoner (1991) interpreted the base of unit TS3 as a sequence boundary at the base of an incised valley (his "sequence boundary 5"), where it has a sharp-to-erosional character to the west of the study area. Willis and Gabel (2001) document a composite erosion surface, formed by amalgamation of multiple erosion surfaces of variable relief, at the same stratigraphic level. The top of unit TS3 has not been assigned any sequence stratigraphic significance in previous studies of outcrops to the west of the study area, although locally preserved intense bioturbation is noted at this stratigraphic level (Van Wagoner 1991; Willis and Gabel 2001).

Wave-dominated unit WS6

Description.--- Unit WS6 consists of a thin (<1 m) interval of distal lower shoreface deposits (FA1) that is present in laterally extensive (up to c. 2 km) lenses in the central and eastern part of the study area (sections 7 and 10 in Fig. 8), and an intensely bioturbated surface capping a tidal-bar and channel-fill succession (FA6, FA7) elsewhere (sections 1-5, 8, 9, and 11 in Fig. 8). Unit WS6 is sharply overlain by tidal-bar and wave-influenced tidal-bar deposits (FA5, FA6; assigned to unit TS4 in Fig. 8), which locally are channelized and erode through unit WS6 (section 6 in Fig. 8). These stratigraphic relationships with unit TS4 are interpreted below.

Tide-dominated unit TS4

Description.--- Tidal-sandstone unit TS4 forms a laterally extensive sheet up to 7 m thick across the entire study area (Fig. 8). The unit comprises tidal-bar and wave-influenced tidal-bar deposits (FA5, FA6) throughout the study area, which locally overlie distal lower shoreface deposits (FA1) assigned to unit WS6 across a sharp-to-erosional basal surface that is lined by a discontinuous mudclast conglomerate (Fig. 8). Wave-influenced tidal-bar deposits (FA5) in the central part of the study area are confined to a belt of laterally stacked channel fills, each of which is c. 350 m wide and 5–7 m deep (between sections 4 and 7 in Figs. 8, 9). Lateral accretion and stacking of the channel fills indicates a progressive northeast-to-southwest shift of the channel axes (between sections 4 and 7 in Figs. 8, 9). Locally, the channel bases have eroded out unit WS6, causing amalgamation of units TS3 and TS4 (section 6 in Fig. 8). Here, the basal surface of unit TS4 is hardly distinguishable from smaller-scale erosional surfaces between and within tidal bars. Paleocurrents are bidirectional, and are locally oriented towards the north and south, or towards the northwest and southeast (Figs. 8, 10E). Unit TS4 is capped by a thin (up to 1 m), *Ophiomorpha*-burrowed sandstone that is overlain by marine shales of the Anchor Mine Tongue.

Interpretation.--- Unit TS4 contains tidal-bar deposits that transition laterally, to both the west and the east, into wave-influenced tidal-bar deposits (Figs. 8, 10E), which is interpreted to represent a proximal-to-distal change in facies association, as in units TS2 and TS3. As for the underlying tide-dominated units, unit TS4 is inferred to have been time-equivalent and genetically linked to wave-dominated unit WS6 (Fig. 10E; cf. Willis & Gabel 2001), and the sharp base of TS4 is attributed to submarine tidal scour during progradation. Lateral facies variation to the west and the east implies an irregular shoreline morphology in plan view, potentially different to the regional shoreline trend (Fig. 1B), while tidal bars are subject to a far greater degree of wave influence than in underlying tide-dominated units. These aspects may reflect decreased tidal amplification and/or decreased wave

attenuation in response to paleogeographic re-organisation of the "lower Sego Delta". Paleocurrents are interpreted to record shore-normal, ebb- and flood-tidal currents, as in units TS2 and TS3. The top of unit TS4 is interpreted to record an increase in water depth, from tidal-bar and wave-influenced tidal-bar deposits to overlying marine shales of the Anchor Mine Tongue, across a flooding surface (FS400; Figs. 6, 8).

Comparison with regional stratigraphic framework.--- Unit TS4 represents the upper part of the "tidal unit overlying sequence boundary 5" of Van Wagoner (1991) to the west of the study area, and is correlative to the upper part of "sandstone 2" of Willis and Gabel (2001) in their "Westwater study area". These previous studies have not assigned any sequence stratigraphic significance to the base of unit TS4 in outcrops to the west of the study area, but the top of unit TS4 (and coincident base of the Anchor Mine Tongue) has been previously interpreted as a flooding surface (Van Wagoner 1991; Willis and Gabel 2001; Hettinger and Kirschbaum 2002; Kirschbaum and Hettinger 2004).

Overall stratigraphic architecture of the distal part of the lower Sego Sandstone

Description.--- The positions of the down-dip termination of successive tidal-sandstone units record pronounced overall progradation (between units TS1 and TS2) followed by aggradation (between units TS2 and TS4) (Figs. 8, 10B-E). Aggradational stacking of units TS2, TS3, and TS4 is accompanied by an increase in the depositional-dip extent of wave-reworked and wave-influenced tidal bar deposits (Figs. 8, 10B-E). The landward limit of wave-reworked and wave-influenced tidal bar deposits moves up depositional dip between units TS3 and TS4, implying retrogradational stacking of these units and/or expansion of the depositional-dip extent of the facies belts represented by the deposits.

Interpretation and comparison with regional stratigraphic framework.--- The stratigraphic architecture described above records overall regression and transgression of the "lower Sego Delta". Maximum regression of the delta is represented by the top of either unit TS3 or unit TS4, but further interpretation of the overall stratigraphic architecture is speculative at best. The pronounced progradation between units TS1 and TS2 may be interpreted as the down-dip correlative of a low-order sequence boundary (occupying the position of "sequence boundary 3" of Van Wagoner et al. 1991). This interpretation would assign units WS4, TS2, WS5, TS3, WS6, and TS4 to a low-order lowstand systems tract, and underlying units WS1, WS2, TS1, and WS3 to a low-order highstand systems tract. The large depositional-dip extent of wave-reworked and wave-influenced tidal bar

772 deposits in units TS2, TS3, and TS4 may then represent enhanced wave influence during overall
773 lowstand conditions, which perhaps peaked during the transgression that resulted in deposition of
774 the Anchor Mine Tongue above unit TS4. There is no systematic stratigraphic variation in the depth
775 of basal erosional scour or facies composition of tidal sandstone units in outcrops to the west of the
776 study area, such that neither Van Wagoner (1991) and (Willis and Gabel 2001) offered a low-order
777 sequence stratigraphic interpretation of the lower Sego Sandstone but instead focussed on high-order
778 sequence architecture. We concur with their approach; low-order sequence stratigraphic
779 interpretations of the lower Sego Sandstone presented to date (e.g. Willis 2000; Aschoff and Steel
780 2011a) have relied on correlations between widely spaced measured sections that assumed a simple
781 model of architecture within high-frequency sequences, which is not supported by detailed outcrop
782 mapping.
783
784 **DISCUSSION**
785
786 The lower Sego Sandstone has previously been interpreted as the deposits of a system that was wave-
787 dominated at some times, and tide-dominated at others. Tidal dominance was interpreted to be
788 present either within lowstand-to-transgressive valley-fill deposits that cut into highstand wave-
789 dominated shoreface deposits (Wagoner 1991; Yoshida et al. 1996; Willis 2000), or within late-
790 highstand-to-lowstand deltaic deposits that are separated by transgressive-to-early-highstand wave-
791 dominated shoreface deposits, due to variations in seaway geometry and associated tidal resonance
792 (Willis and Gabel 2001). In contrast to these previous interpretations of the lower Sego Sandstone
793 from relatively proximal settings, in this paper we document evidence for the simultaneous action of
794 tide and wave processes within the distal part of the "lower Sego Delta". In this section, we present a
795 depositional model based on this evidence, and discuss its wider implications for sedimentologic and
796 sequence-stratigraphic interpretation of similar mixed tide- and wave-influenced deltaic deposits.
797
798 ***Depositional model for distal lower Sego Sandstone***
799
800 Tidal bars and channel fills (FA6-FA8) are the main architectural elements in proximal deposits (units
801 TS1-TS4), which thin and transition down depositional dip into wave-dominated deposits (units WS
802 1-5) (Fig. 8). This change reflects the transition from the proximal part of tidal distributary mouth bars
803 towards their distal parts, where waves are increasingly active (Dalrymple and Choi 2007), and does
804 not occur across a sequence-stratigraphic surface. Although waves were also active in more proximal
805 parts of the delta front, tidal currents were strong enough to rework most wave-generated structures

(left panel in Fig. 11). Further seaward, tidal currents were less confined and thus weaker, and tidal bars were less protected from wave action, resulting in localized reworking and preservation of sedimentary structures generated by waves at bar tops (center panel in Fig. 11). Migration of scour pools in front of tidal bars and superimposed dunes resulted in the development of erosion surfaces separating trough and planar cross-bedded, tidal sandstones above from wave-reworked bar-top deposits below (center panel in Fig. 11). The greatest degree of mixed tide and wave influence occurs in facies associations that record the outer, seaward-lying parts of tidal bars (FA4, FA5; Figs. 3F-G, 4), and in tidally modulated, wave-dominated shoreface deposits (FA 3; Fig. 3C-E) that occur locally in more distal locations (center and right panels in Fig. 11). Wave-ripple cross-lamination is rare, and predominantly storm-wave-generated structures, such as HCS, are rarely intercalated within tidal bar deposits. The outer, seaward-lying parts of tidal bars are envisaged to have been reworked by storm waves that eroded their tops (FA5), and transported and redeposited sand in wide shoals lying paleoseaward of the pinchout of tidal deposits (FA4) to leave behind broad, low relief bars (Fig. 11). Where storm-wave reworking of the outer parts of the bars was subject to little scour during dune migration in response to tidal currents, bed-scale intercalations of tidal cross-sets and hummocky cross-stratified storm-event beds are preserved (Figs. 4B-D; 11). Elsewhere, prograding tidal bars and their component dunes erosionally scoured into underlying wave-dominated deposits, resulting in sharp-based tidal bars juxtaposed above wave-dominated shoreface deposits across planar and low-relief erosion surfaces. The effectiveness of storm-wave reworking was variable; it appears to have been absent near the down-dip pinchout of unit TS1, where tidal bar deposits (FA6) pass directly an relatively abruptly into wave-dominated lower shoreface deposits (FA2), but far more pronounced in units TS2, TS3, and TS4, in which tidal bar deposits (FA6) pass gradually down dip into wave-influenced and wave-reworked tidal bar deposits (FA4, FA5). Such variability may reflect the influence of local bathymetry, which controlled the orientation of ebb- and flood-tidal currents relative to the direction of wave approach, and/or regional paleogeography, which controlled the degree of tidal amplification and wave attenuation. The distribution of interpreted tidally modulated, wave-dominated proximal lower shoreface deposits (FA 3), in which HCS records variations in water depth over one or more tidal cycles, is localized in the lower Sego Sandstone. Similar tidal modulation of storm-event beds has been documented on open-coast tidal flats (Yang et al. 2008) and shorefaces fringing large embayments (Dashtgard et al. 2009, 2012), both developed under macrotidal conditions. The patchy distribution of tidally modulated, wave-dominated proximal lower shoreface deposits in the lower Sego Sandstone may have resulted from a smaller tidal range and/or localized variability in the gradient and lateral extent of the lower shoreface.

Overall, the distal tidal deposits of the Lower Sego Sandstone (FA6-FA8 in units TS1-TS4; Fig. 8) show many similarities to tidal distributary mouth bars and outer estuarine bars (cf. Dalrymple and Choi 2007). Tidal indicators including thin mud drapes and reactivation surfaces are common. Paleocurrent directions are bidirectional at any one location in the study area, and ebb-directed currents dominated (Fig. 8). However, fluid mud deposits that typify modern tide-dominated deltas (e.g. Fly River Delta; Harris et al. 1993) are absent from the base of channels, and the overall mud content is low, implying a combination of deposition outside the tidal maximum zone and offshore transport of mud by wave reworking. Laterally accreting fining-upward bars represent the infill of active tidal distributary channels (FA7 in Figs. 7, 12) and the inclination of lateral accretion surfaces decreases down depositional dip implying that channels and bars became wider and their height decreased down depositional dip. Channel abandonment resulted in localized interruption of sand delivery. Mud was transported into the abandoned channel by flood-dominated tidal currents and the establishment of normal marine salinities allowed intense bioturbation (FA8 in Figs. 7, 12). Tidal bars are characterized by thickening-upwards trends, and overlie wave-dominated shoreface deposits on the delta front (FA6 in Figs. 7, 12). Tidal bars show increasing wave influence in their outer parts, where they were subjected to storm-wave reworking (FA4 and FA5 in Figs. 7, 12), and pass gradationally seaward into wave-dominated shoreface deposits (FA1, FA2, and FA3 in Figs. 7, 12).

The degree of wave influence shows some stratigraphic variation, and is greater locally at or directly below the flooding surfaces that cap each tide-dominated unit (TS1-TS4, Fig. 8), suggesting an increase in wave action relative to tidal action during flooding of tidal bars and channels (cf. Van Wagoner, 1991; Willis and Gabel, 2001), for reasons outlined below. This effect is most pronounced at the top of the lower Sego Sandstone (below FS400 at the top of unit TS4, Fig. 8), which is associated with a major landward displacement of the shoreline at the base of the Anchor Mine Tongue.

In a regional paleogeographic context, the "lower Sego Delta" built out towards the mouth of a sheltered embayment (Utah Bight in Fig. 1A) during progradation, such that deposition may have become increasingly wave influenced from up regional depositional dip (northwest) to down regional depositional dip (southeast). This scenario is comparable to that of the Holocene Mekong Delta, which developed from tide-dominated to mixed wave-and-tide-influenced after migrating past a headland which previously protected the delta from storm waves and longshore currents (Ta et al. 2005). The sheltering effect invoked in this scenario was reduced during deposition of the uppermost part of the lower Sego Sandstone (unit TS4; Fig. 8), resulting in stronger relative wave influence throughout the study area prior to major flooding and deposition of the Anchor Mine Tongue.

Increased relative wave influence may have resulted from paleogeographic re-organisation of the "lower Sego Delta" due to large-scale avulsion of trunk deltaic distributaries, and/or subtle tectonically induced changes in seafloor bathymetry (cf. Aschoff and Steel 2011a; Steel et al. 2012). Approximately time-equivalent strata of the Sego Sandstone in northwest Colorado, c. 100 km north of the study area, are interpreted to contain the deposits of barrier island systems (York et al. 2011; Painter et al. 2013), implying a microtidal to mesotidal regime in the Utah Bight (Fig. 1A).

Implications for sequence-stratigraphic interpretation of mixed, tide-and-wave-influenced deltaic deposits

Our interpretation of the distal part of the lower Sego Sandstone as the deposits of a mixed tide- and wave-influenced delta implies that waves and tides operated in tandem during delta deposition, but were effective in transporting and reworking sediment in different water depth ranges and at different geographic locations. As a result, most facies associations and stratigraphic units tend to be either wave-dominated (FA1, FA2 in units WS1-WS6; Figs. 8, 10) or tide-dominated (FA6, FA7, and FA8 in units TS1-TS4; Figs. 8, 10), although the overall system was of mixed influence. Similar spatial partitioning of tide-dominated and wave-dominated deposits has been noted in other regressive, tide-influenced deltaic deposits (e.g. Prave et al. 1996; Mellere and Steel 1995; Seidler and Steel 2001) and net-transgressive shallow-marine strata of mixed influence (e.g. Hendricks 1994; Sixsmith et al. 2008). In some cases, spatial partitioning of tide-dominated and wave-dominated deposits in regressive deltaic deposits has been attributed to a temporal change in process regime (Mellere and Steel 1995, 2000), including in the proximal part of the lower Sego Sandstone (e.g. Wagoner 1991; Yoshida et al. 1996; Willis 2000; Willis and Gabel 2001). In this interpretation, wave-dominated deposits are assigned to highstand or falling-stage systems tracts, and overlying tide-dominated deposits are assigned to lowstand systems tracts. The contacts between wave-dominated deposits and overlying tide-dominated deposits are interpreted as sequence boundaries, based on an interpreted offlapping or downstepping stratal architecture, although the contact itself is locally sharp-to-transitional (Mellere and Steel 1995, 2000; Seidler and Steel 2001) or deeply erosional in character (Wagoner 1991; Willis and Gabel 2001, 2003). Alternatively, spatial partitioning of tide-dominated and wave-dominated deposits has been interpreted to reflect geographic variations in process dominance (Duke et al. 1991; Prave et al. 1996), as in our interpretation of the distal part of the lower Sego Sandstone. The contacts between wave-dominated deposits and overlying tide-dominated deposits are documented to be sharp to slightly erosional (<0.5 m relief), but neither sediment texture nor interpreted water depths indicate an abrupt basinward facies shift (Duke et al. 1991; Prave et al. 1996).

908 Interbedded tide-dominated and wave-dominated deposits similar to those noted in FA5 (Fig. 4) have
909 previously been documented in mixed-influence delta-front strata, but only near the down-dip
910 termination of regressive-transgressive tongues similar to those described herein (Willis et al. 1999;
911 Bhattacharya and Willis 2001; Gani and Bhattacharya 2007). In tide-dominated deltaic deposits with
912 only minor wave influence, sporadic wave ripples occur in the distal delta front and in abandoned
913 estuarine channel fills (Maguregui and Tyler 1991).
914
915 The partitioning of tide-dominated and wave-dominated deposits, and thus the apparent partitioning
916 of processes, in the distal part of the lower Sego Sandstone, results from the potential for tidal
917 currents to completely rework wave-dominated deposits on the proximal part of the delta front (cf.
918 Pontén and Plink-Björklund 2009), and the potential for storm waves to completely rework tide-
919 dominated deposits on the distal part of the delta front (Fig. 11). Additionally, tidal scour during
920 delta progradation resulted in removal of mixed, tide-and-wave-influenced deposits (FA3, FA4, FA5)
921 in the much of the distal part of the lower Sego Sandstone. Tide-and-wave-influenced deposits (FA3,
922 FA4, FA5) are only rarely preserved near the base and, particularly, down-dip pinchout of regressive-
923 transgressive tongues in the distal part of the lower Sego Sandstone. The resulting spatial partitioning
924 of tide-dominated and wave-dominated facies associations is documented herein only near the down-
925 dip termination of regressive-transgressive tongues in the lower Sego Sandstone, close to their
926 "regressive-transgressive turnaround", although it can also be readily used to re-interpret the
927 stratigraphic architectures documented in more proximal parts of each tongue (e.g. Wagoner 1991;
928 Willis and Gabel 2001). Such spatial partitioning of process-specific facies associations has profound
929 implications for interpreting the stratigraphic record.
930
931 Simple sequence stratigraphic models that assign wave-dominated deposits to regression and tide-
932 dominated deposits to transgression (e.g. Van Wagoner et al. 1990; Van Wagoner 1991; Cross et al.
933 1993), and more sophisticated models that relate changes in process regime to relative sea-level and
934 basin bathymetry (e.g. Willis and Gabel 2001; Yoshida et al. 2007; Ainsworth et al. 2008) may both be
935 misleading if uncritically applied. Such models may be taken to provide a rationale for interpreting
936 key sequence stratigraphic surfaces (e.g. sequence boundaries, flooding surfaces) at contacts between
937 tide-dominated and wave-dominated deposits in the absence of interpreted trends in water depth,
938 and resulting correlations are likely to be inappropriate for mixed-influence depositional systems.
939 Instead, robust sequence stratigraphic interpretations must incorporate the change from tide-
940 dominated deposits in a specific range of water depths and geographic locations (e.g. tidal bar and
941 channel-fill deposits, FA6-FA8, representing water depths that were generally above fair-weather

wave base in the lower Sego Sandstone) to wave-dominated deposits in a different range of water depths and locations (e.g. lower shoreface deposits, FA1-FA2, representing water depths between storm wave base and fair-weather wave base) (Prave et al. 1996). In sparse core datasets from the subsurface, this will require interpretation of vertical trends in water depth via careful facies analysis, supported by contextual paleogeographic data that allow interpretation of an overall mixed-influence depositional system (cf. tide-influenced, fluvial-dominated delta interpreted by Pontén and Plink-Björklund 2007). The greatest challenge in adopting this approach in general is the paucity of process- and facies-based criteria for interpreting water depth and proximal-to-distal trends in depositional systems of mixed wave-, tide-, and river-influence (e.g. Hampson et al. 2008), despite the predominance of such depositional systems along modern shorelines and, probably, in ancient strata (Ainsworth et al. 2012; Vakarelov and Ainsworth 2013). For example, tidal currents may act across a wide range of water depths, depending on the shape and size of the tidal basin, and the detailed bathymetric and paleogeographic context of particular locations within it (Johnson and Belderson 1969). In the case of the distal part of the lower Sego Sandstone, tidal-current action was prevalent in shallow water, approximately above fair-weather wave base, whereas storm-wave action dominated in deeper water, between storm wave base and fair-weather wave base. However, the low abundance of mud in the lower Sego Sandstone suggests extensive offshore transport by waves (Fig. 11), and provides indirect evidence for wave influence even in tide-dominated parts of the depositional system (cf. Eocene Roda Sandstone, Spain, López-Blanco et al. 2003).

CONCLUSIONS

The Upper Cretaceous lower Sego Sandstone has been studied near its down-dip pinchout in the Book Cliffs, western Colorado, USA, in order to document facies characteristics and stratigraphic relationships in the distal part of an ancient, mixed wave-and-tide-influenced deltaic succession. The lower Sego Sandstone comprises four vertically stacked, regressive-transgressive tongues bounded by flooding surfaces. The proximal part of each regressive-transgressive tongue contains tide-dominated sandstones that sharply to erosionally overlie, and laterally interfinger with, wave-dominated deposits in the distal part of the tongue.

Tide-dominated sandstones are fine- to medium-grained, and comprise the deposits of tidal bars and tide-dominated distributary channels developed on the proximal part of the delta front. Tidal bar deposits (facies association FA6) are characterized by coarsening-upward successions of wavy bedded and cross-bedded sandstones containing abundant mud drapes, reactivation surfaces and

bidirectional paleocurrent indicators. Active tide-dominated distributary channel fills (FA7) comprise similar lithologic components arranged within fining-upward successions that contain heterolithic lateral accretion deposits at their margins. The lithologic similarity of tidal-bar and adjacent distributary channel-fill deposits implies that active channel filling occurred by lateral bar migration. Abandoned distributary channel fills (FA8) comprise intensely bioturbated mudstones.

Wave-dominated deposits (FA1, FA2) consist of coarsening-upward successions of mudstone and intercalated HCS-bearing, very fine- to fine-grained sandstone beds that represent storm events. These deposits represent deposition in wave-dominated lower shoreface environments on the distal part of the delta front. Rhythmic variations in the wavelength of HCS within some, localized successions (FA3) may record tidal modulation of water depth and storm-wave velocities over one or more tidal cycles.

Direct, bed-scale evidence for mixed tide and wave influence occurs at the lateral, proximal-to-distal transition from tide-dominated sandstones (FA6-FA8) to wave-dominated deposits (FA1, FA2). Here, deposits of the outer, seaward-lying parts of tidal bars (FA5) contain HCS-bearing, very fine-grained sandstone beds intercalated with cross-bedded, fine- to medium-grained sandstones containing tidal indicators. Fine-grained, low-angle cross-stratified and HCS-bearing sandstones of similar grain size and texture (FA4) occur in more distal, conjoined locations, and are interpreted as tidal bar deposits that were completely reworked by storm waves.

In combination, these facies components and their architectural arrangement suggest that waves and tides operated in tandem throughout deposition of the "lower Sego Delta". The spatial partitioning of tide-dominated and wave-dominated deposits into, respectively, the proximal and distal parts of each regressive-transgressive tongue suggests that tides and waves were effective in transporting and reworking sediment in different water depth ranges and at different geographic locations. Mixed tide-and-wave-influenced deposits (FA3, FA4, FA5) are only rarely preserved near the base and, particularly, down-dip pinchout of regressive-transgressive tongues in the lower Sego Sandstone; elsewhere they are removed by tidal scour during delta progradation. The spatial partitioning of process-specific, but time-equivalent, facies associations may have profound implications for sequence stratigraphic interpretation of shallow-marine deposits of mixed process influence. For example, sharp-to-erosional juxtapositions of tide-dominated sandstones above wave-dominated deposits in the distal part of the lower Sego Sandstone do not record sequence boundaries separating highstand deposits from overlying lowstand-to-transgressive valley-fill deposits. Neither does a

temporal change in process regime, for example due to variations in tidal resonance controlled by basin geometry, need to be invoked to explain the vertical juxtaposition. Instead, these architectural relationships can be readily explained in a single, time-invariant depositional model.

ACKNOWLEDGEMENTS

Funding of this work, and approval for publication by Shell Norway, Statoil, Total and Petoro are gratefully acknowledged. Field work would not have been possible without the assistance of Virginia Stacey, Ruairi McDonald, and Gavin Graham. We also thank Kyungsik Choi, Robert Dalrymple, Brian Willis, Lesli Wood, and Byongcheon Yang for thought-provoking discussions of aspects of the work presented here. We are grateful for the constructive reviews and editorial comments of Janok Bhattacharya, Howard Feldman, and Brian Willis.

REFERENCES

Ainsworth, R.B., Flint, S.S., and Howell, J.A., 2008, Predicting coastal depositional style: influence of basin morphology and accommodation to sediment supply ratio within a sequence stratigraphic framework, *in* Hampson, G.J., Steel, R.J., Burgess, P.M., and Dalrymple, R.W., eds., Recent advances in models of siliciclastic shallow-marine stratigraphy: SEPM, Special Publication 90, p. 237-263.

Ainsworth, R.B., Vakarelov, B.K., and Nanson, R.A., 2011, Dynamic spatial and temporal prediction of changes in depositional processes on clastic shorelines: toward improved subsurface uncertainty reduction and management: American Association of Petroleum Geologists, Bulletin, v. 95, p. 267–297.

Allen, G.P. and Chambers, J.L.C., 1998, Sedimentation in the modern and Miocene Mahakam Delta: Indonesian Petroleum Association, Jakarta, Indonesia, 231 p.

Aschoff, J.L., and Steel, R.J., 2011a, Anatomy and development of a low-accommodation clastic wedge, upper Cretaceous, Cordilleran Foreland Basin, USA: Sedimentary Geology, v. 236, p. 1–24.

Aschoff, J.L., and Steel, R.J., 2011b, Anomalous clastic wedge development during the Sevier-Laramide transition, North American Cordilleran foreland basin, USA: Geological Society of America, Bulletin, v. 123, p. 1822–1835.

Bhattacharya, J.P., and Willis, B.J., 2001, Lowstand eltas in the Frontier Formation, Powder River Basin, Wyoming: implications for sequence stratigraphic models: American Association of Petroleum Geologists, Bulletin, v. 85, p. 261-294.

Bromley, R.G, Pemberton, S.G., and Rahmani, R.A., 1984, A Cretaceous woodground: the *Teredolites* ichnofacies: Journal of Paleontology, v. 58, p. 488-498.

Burton, D. and Wood, L.J., 2011, Quantitative shale characterization of the tidally influenced Sego Sandstone: American Association of Petroleum Geologists, Bulletin, v. 95, p. 1207–1226.

Cross, T.A., Baker, M.R., Chapin, M.A., Clark, M.S., Gardner, M.A., Hanson, M.S., Lessenger, M.A., Little, L.D., McDonough, K.-J., Sonnenfeld, M.D., Valasek, D.W., Williams, M.W., and Witter, D.N., 1993, Applications of high-resolution sequence stratigraphy to reservoir analysis, *in* Eschard, R., and Doligez, B., eds., Subsurface reservoir characterization from outcrop observations: Éditions Technip, Paris, p. 11-33.

Dalrymple, R.W., and Choi, K., 2007, Morphologic and facies trends through the fluvial-marine transition in tide-dominated depositional systems: a schematic framework for environmental and sequence-stratigraphic interpretation: Earth-Science Reviews, v. 81, p. 135-174.

Dalrymple, R.W., and Rhodes, R.N., 1995, Estuarine dunes and bars, *in* Perillo, G.M.E., ed., Geomorphology and sedimentology of estuaries: Elsevier, Amsterdam, p. 359–422.

Dashtgard, S.E., Gingras, M.K., and MacEachern, J.A., 2012, Tidally modulated shorefaces: Journal of Sedimentary Research, v. 79, p. 793-807.

Dashtgard, S.E., MacEachern, J.A., Frey, S.E., and Gingras, M.K., 2012, Tidal effects on the shoreface: towards a conceptual framework: Sedimentary Geology, v. 279, p. 42-61.

Dott, R.H., and Bourgeois, J., 1982, Hummocky stratification: significance of its variable bedding sequences: Geological Society of America Bulletin, v. 93, p. 663-680.

Duke, W.L., 1985, Hummocky cross stratification, tropical hurricanes, and intense winter storms: Sedimentology, v. 32, p. 167-194.

Duke, W.L., Fawcett, P.J., and Brusse, W.C., 1991, Prograding shoreline deposits in the Lower Silurian Medina Group, Ontario and New York; storm- and tide-influenced sedimentation in a shallow epicontinental sea, and the origin of enigmatic shore-normal channels encapsulated by open shallow-marine deposits, *in* Swift, D.J.P., Oertel, G.F., Tillman, R.W., and Thorne, J.A., eds., Shelf sand and sandstone bodies: geometry, facies and sequence stratigraphy*:* International Association of Sedimentologists, Special Publication 14, p. 339-375.

Dumas, S., Arnott, R.W.C., and Southard, J.B., 2005. Experiments on oscillatory-flow and combined-flow bed forms: implications for interpreting parts of the shallow-marine sedimentary record: Journal of Sedimentary Research, v. 75, p. 501-513.

Erdmann, C.E., 1934, The Book Cliffs coal field in Garfield and Mesa Counties, Colorado: U.S. Geological Survey Bulletin, v. 851, 150 p.

Ericksen, M.C., and Slingerland, R., 1990, Numerical simulations of tidal and wind-driven circulation in the Cretaceous Interior Seaway of North America: Geological Society of America, Bulletin, v. 102, p. 1499–1516.

Fisher, D.J., 1936, The Book Cliffs coal field in Emery and Grand Counties, Utah: U.S. Geological Survey Bulletin, v. 852, 104 p.

Fisher, D.J., Erdmann, C.E., and Reeside, J.B., Jr., 1960, Cretaceous and Tertiary formations of the Book Cliffs, Carbon, Emery, and Grand Counties, Utah, and Garfield and Mesa Counties, Colorado: U.S. Geological Survey, Professional Paper 332, 80 p.

Fouch, T.D., Lawton, T.F., Nichols, D.J., Cashion, W.B., and Cobban, W.A., 1983, Patterns and timing of synorogenic sedimentation in Upper Cretaceous rocks of central and northeast Utah, *in* Reynolds, M.W., and Dolly, E.D., eds., Mesozoic paleogeography of the west-central United States: SEPM, Rocky Mountain Section, Denver, Colorado, p. 305-336.

Franczyk, K.J., 1989, Depositional controls on the late Campanian Sego Sandstone and implications for associated coal-forming environments in the Uinta and Piceance basins: U.S. Geological Survey, Bulletin, v. 1787-F, p. F1-F17.

Franczyk, K.J., Pitman, J.K., and Nichols, D.J., 1990, Sedimentology, mineralogy, palynology, and depositional history of some uppermost Cretaceous and lowermost Tertiary rocks along the Utah Book and Roan cliffs east of the Green River: U.S. Geological Survey Bulletin, v. 1787-N, p. N1-N27.

Gani, M.R., and Bhattacharya, J.P., 2007, Basic building blocks and process variability of a cretaceous delta: internal facies architecture reveals a more dynamic interaction of river, wave, and tidal processes than is indicated by external shape: Journal of Sedimentary Research, v. 77, p. 284-302.

Hampson, G.J., Procter, E.J., and Kelly, C., 2008, Controls on isolated shallow-marine sandstone deposition and shelf construction: Late Cretaceous Western Interior Seaway, northern Utah and Colorado, *in* Hampson, G.J., Steel, R.J., Burgess, P.M., and Dalrymple, R.W., eds., Recent advances in models of siliciclastic shallow-marine stratigraphy: SEPM, Special Publication 90, p. 355-389.

Harris, P.T., Baker, E.K., Cole, A.R., and Short, S.A., 1993, A preliminary study of sedimentation in the tidally dominated Fly River delta, Gulf of Papua: Continental Shelf Research, v. 13, p. 441–472.

Hendricks, M.L., 1994, Ravinement surface control on hydrocarbon accumulation in transgressive systems tracts: Almond Formation, Green River Basin, Wyoming, *in:* Dolson, J.C., Hendricks, M.L., and Westcott, W.A., eds., Unconformity-related hydrocarbons in sedimentary sequences: Rocky Mountain Association of Geologists, p. 209-218.

Hettinger, R.D., and Kirschbaum, M.A., 2002, Stratigraphy of the Upper Cretaceous Mancos Shale (Upper Part) and Mesaverde Group in the southern part of the Uinta and Piceance Basins, Utah and Colorado: U.S. Geological Survey, Geologic Investigations Series I-2764.

Houbolt, J.J.H.C., 1968, Recent sediments in the Southern Bight of the North Sea: Geologie en Mijnbouw, v. 47, p. 245-273.

Johnson, M.A., and Belderson, R.H., 1969, The tidal origin of some vertical sedimentary changes in epicontinental seas: Journal of Geology, v. 77, p. 353-357.

Kauffman, E.G., and Caldwell, W.G.E., 1993, The Western Interior Basin in space and time, *in* Caldwell, W.G.E., and Kauffman, E.G., eds., Evolution of the Western Interior Basin: Geological Association of Canada, Special Paper 39, p. 1-30.

Kineke, G.C., Sternberg, R.W., Trowbridge, J.H., and Geyer, W.R., 1996, Fluid-mud processes on the Amazon continental shelf: Continental Shelf Research, v. 16, p. 667-696.

Kirschbaum, M.A., and Hettinger, R.D., 2004, Facies analysis and sequence stratigraphic framework of Upper Campanian strata (Neslen and Mount Garfield Formations, Bluecastle Tongue of the Castlegate Sandstone, and Mancos Shale), Eastern Book Cliffs, Colorado and Utah: U.S. Geological Survey, Digital Data Series DDS-69-G (CD-ROM only).

Krystinik, L.F., and DeJarnett, B.B., 1995, Lateral variability of sequence stratigraphic framework in the Campanian and Lower Maastrichtian of the Western Interior Seaway, *in* Van Wagoner, J.C., and Bertram, G.T., eds., Sequence stratigraphy of foreland basin deposits: outcrop and subsurface examples from the Cretaceous of North America: American Association of Petroleum Geologists, Memoir 64, p. 11-26.

Liu, S., Nummedal, D., and Liu, L., 2011, Migration of dynamic subsidence across the Late Cretaceous United States Western Interior Basin in response to Farallon plate subduction: Geology, v. 39, p. 555-558.

Liu, S., Nummedal, D., and Gurnis, M., 2014, Dynamic versus flexural controls of Late Cretaceous Western Interior Basin, USA: Earth and Plantary Science Letters, v. 389, p. 221-239.

López-Blanco, M., Marzo, M., and Muñoz, J.A., 2003, Low-amplitude, synsedimentary folding of a deltaic complex: Roda Sandstone (lower Eocene), South-Pyrenean Foreland Basin: Basin Research, v. 15, p. 73–95.

MacEachern, J.A., and Bann, K.L., 2008, The role of ichnology in refining shallow marine facies models, *in* Hampson, G.J., Steel, R.J., Burgess, P.M., and Dalrymple, R.W., eds., Recent advances in models of siliciclastic shallow-marine stratigraphy: SEPM, Special Publication 90, p. 73-116.

MacQuaker, J.H.S., Bentley, S.J., and Bohacs, K.M., 2010, Wave-enhanced sediment-gravity flows and mud dispersal across continental shelves: reappraising sediment transport processes operating in ancient mudstone successions: Geology, v. 38, p. 947-950.

Maguregui, J., and Tyler, N., 1991, Evolution of middle Eocene tide-dominated deltaic sandstones, Lagunillas Field, Maracaibo Basin, western Venezuela, *in* Miall, A.D., and Tyler, N., eds., The three-dimensional architecture of terrigenous clastic sediments, and its implications for hydrocarbon discovery and recovery: SEPM, Concepts in Sedimentology and Paleontology, v. 3, p. 233–244.

Martinsen, R.S., 2003, Depositional remnants, part 2: examples from the Western Interior Cretaceous basin of North America: American Association of Petroleum Geologists, Bulletin, v. 87, p. 1883-1909.

McGookey, D.P., Haun, J.P., Heele, L.A., Goodell, H.G., McCubbin, D.G., Wiemer, R.J., and Wulf, G.R., 1972, Cretaceous system, *in* Mallory, W.W., ed., Geologic map of the Rocky Mountain region: Rocky Mountain Association of Geologists, p. 190-233.

McLaurin, B.T., and Steel, R.J., 2000, Fourth-order nonmarine to marine sequences, middle Castlegate Formation, Book Cliffs, Utah: Geology, v. 28, p. 359–362.

Mellere, D., and Steel, R.J, 1995, Facies architecture and sequentiality of nearshore and 'shelf' sandbodies; Haystack Mountains Formation, Wyoming, USA: Sedimentology, v. 42, p. 551-574.

Mellere, D., and Steel, R.J, 2000, Style contrast between forced regressive and lowstand/transgressive wedges in the Campanian of south-central Wyoming (Hatfield Member of the Haystack Mountains Formation), *in* Hunt, D., and Gawthorpe, R.L., eds., Sedimentary responses to forced regression: Geological Society of London, Special Publication 172, p. 141-162.

Michels, K.H., Kudrass, H.R., Hübscher, C., Suckow, A., and Wiediecke, M., 1998, The submarine delta of the Ganges–Brahmaputra: cyclone-dominated sedimentation patterns: Marine Geology, v. 149, p. 133–154.

Mutti, E., Rosell, J., Allen, G.P. and Sgavetti, M., 1985, The Eocene Baronia tide dominated delta-shelf system in the Ager Basin), *in* Mila, M.D., and Rosell, J., eds., Excursion Guidebook, 6th European regional Meeting: International Association of Sedimentologists, Lleida, Spain, p. 579-600.

Nesbitt, E.A. and Campbell, K.A., 2002, A new *Psilonichnus* ichnospecies attributed to mud-shrimp *Upogebia* in estuarine settings: Journal of Paleontology, v. 76, p. 892–901.

Nesbitt, E.A. and Campbell, K.A., 2006, The paleoenvironmental significance of *Psilonichnus*: Palaois, v. 21, p. 187–196.

Nio, S.-D., and Yang, C., 1991, Diagnostic attributes of clastic tidal deposits; a review, *in* Smith, D.G., Zaitlin, B.A., Reisnon, G.E., and Rahmani, R.A., eds., Clastic tidal sedimentology: Canadian Society of Petroleum Geologists, Memoit 16, p. 3-27.

Nummedal, D., and Riley, G.W., 1999, The origin of the Tocito Sandstone and its sequence stratigraphic lessons, *in* Bergman, K.M., and Snedden, J.W., eds., Isolated shallow marine sand bodies: sequence stratigraphic analysis and sedimentologic interpretation: SEPM Special Publication 64, p. 227-254.

Painter, C.S., York-Soweke, C.C., and Carrapa, B., 2013, Sequence stratigraphy of the Upper Cretaceous Sego Sandstone Member reveals spatio-temporal changes in depositional processes, northwest Colorado, USA: Journal of Sedimentary Research, v. 83, p. 323-338.

Parrish, J.T., Gaynor, G.C., and Swift, D.J.P., 1984, Circulation in the Cretaceous Western Interior Seaway of North America, a review, *in* Stott, D.F., and Glass, D.J., eds., The Mesozoic of Middle North America: Canadian Society of Petroleum Geologists, Memoir 9, p. 221-231.

Pontén, A., and Plink-Björklund, P., 2007, Depositional environments in an extensive tide-influenced delta plain, Middle Devonian Gauja Formation, Devonian Baltic Basin: Sedimentology, v. 54, p. 969–1005.

Pontén, A., and Plink-Björklund, P., 2009, Regressive to transgressive transits reflected in tidal bars, Middle Devonian Baltic Basin: Sedimentary Geology, v. 218, p. 48–60.

Prave, A.R., Duke, W.L., and Slattery, W., 1996, A depositional model for storm-and tide-influenced prograding siliciclastic shorelines from the Middle Devonian of the central Appalachian foreland

basin, USA: Sedimentology, v. 43, p. 611-629.

Roberts, L.N.R., and Kirschbaum, M.A., 1995, Paleogeography of the Late Cretaceous of the Western Interior of middle North America – coal distribution and sediment accumulation: United States Geological Survey, Professional Paper 1561, p. 1–115.

Seidler, L., and Steel, R.J., 2001, Pinch-out style and position of tidally infuenced strata in a regressive-transgressive wave-dominated deltaic sandbody, Twentymile Sandstone, Mesaverde Group, NW Colorado: Sedimentology, v. 48, p. 399–414.

Sixsmith, P.J., Hampson, G.J., Gupta, S., Johnson, H.D., and Fofana, J.J., 2008, Facies architecture of a net transgressive sandstone reservoir analog: the Cretaceous Hosta Tongue, New Mexico American Association of Petroleum Geologists, Bulletin, v. 92, p. 513-547.

Slingerland, R., and Keen, T.R., 1999, Sediment transport in the Western Interior Seaway of North America: predictions from a climate-ocean-sediment model, *in* Bergman, K.M., and Snedden, J.W., eds., Isolated shallow marine sand bodies: sequence stratigraphic analysis and sedimentologic interpretation: SEPM Special Publication 64, p. 179-190.

Steel, R.J., Plink-Björklund, P., and Aschoff, J.L., 2012, Tidal deposits of the Campanian Western Interior Seaway, Wyoming, Utah and Colorado, USA, *in* Davis Jr., R.A., and Dalrymple, R.W., eds., Principles of tidal sedimentology: Dordrecht, Springer, p. 437-471.

Storms, J.E.A., and Hampson, G.J., 2005, Mechanisms for forming discontinuity surfaces within shoreface-shelf parasequences: sea level, sediment supply or wave regime?: Journal of Sedimentary Research, v. 75, p. 67-81.

Ta, T.K.O., Nguyen, V.L., Tateishi, M., Kobayashi, I., and Saito, Y., 2005, Holocene delta evolution and depositional models of the Mekong River Delta, southern Vietnam, *in* Giosan, L., and Bhattacharya, J.P., eds., River deltas – concepts, models, and examples: SEPM, Special Publication 83, p. 453-466.

Tänavsuu-Milkeviciene, K., and Plink-Björklund, P., 2009, Recognizing tide-dominated versus tide-influenced deltas: Middle Devonian Strata of the Baltic Basin: Journal of Sedimentary Research, v. 79, p. 887–905.

Vakarelov, B.K., and Ainsworth, R.B., 2013, A hierarchical approach to architectural classification in marginal-marine systems: bridging the gap between sedimentology and sequence stratigraphy: American Association of Petroleum Geologists, Bulletin, v. 97, p. 1121–1161.

Vakarelov, B.K., Ainsworth, R.B., and MacEachern, J.A., 2012, Recognition of wave-dominated, tide-influenced shoreline systems in the rock record: variations from a microtidal shoreline model: Sedimentary Geology, v. 279, p. 23-41.

Van Wagoner, J.C., 1991, High-frequency sequence stratigraphy and facies architecture of the Sego Sandstone in the Book Cliffs of western Colorado and eastern Utah, *in* Van Wagoner, J.C., Nummedal, D., Jones, C.R., Tayloer, D.R., Jennette, D.C., and Riley, G.W., eds., Sequence stratigraphy applications to shelf sandstone reservoirs: outcrop to subsurface examples: American Association of Field Geologists, Field guidebook, Day 1, unpaginated.

Van Wagoner, J.C., Mitchum, R.M., Campion, K.M., and Rahmanian, V.D., 1990, Siliciclastic sequence stratigraphy in well logs, cores, and outcrops: Association of Petroleum Geologists, Methods in Exploration 7, 55 p.

Whitaker, J. H., 1973, "Gutter casts", a new name for scour-and-fill structures; with examples from Llandoverian of Ringerike and Malmoya, southern Norway: Norsk Geologisk Tidsskrift, v. 53, p. 403-417.

Willis, A., 2000, Tectonic control of nested sequence architecture in the Sego Sandstone, Neslen Formation and Upper Castlegate Sandstone (Upper Cretaceous), Sevier Foreland Basin, Utah, USA: Sedimentary Geology, v. 136, p. 277–317.

Willis, B.J., 2005, Deposits of tide-influenced river deltas, *in* Giosan, L., and Bhattacharya, J.P., eds., River deltas – concepts, models, and examples: SEPM, Special Publication 83, p. 87–129.

Willis, B.J., and Gabel, S., 2001, Sharp-based tide-dominated deltas of the Sego Sandstone, Book Cliffs, Utah, USA: Sedimentology, v. 48, p. 479–506.

1312 Willis, B.J., and Gabel, S., 2003, Formation of deep incisions into tide-dominated river deltas:
1313 implications for the stratigraphy of the Sego Sandstone, Book Cliffs, Utah, USA: Journal of
1314 Sedimentary Research, v. 73, p. 246–263.
1315
1316 Willis, B.J., Bhattacharya, J.P., Gabel, S., and White, C.D., 1999, Architecture of a tide-influenced river
1317 delta in the Frontier Formation of central Wyoming, USA: Sedimentology, v. 46, p. 667-688.
1318
1319 Wood, L.J., 2004, Predicting tidal sand reservoir architecture using data from modern and ancient
1320 depositional systems, *in* Grammer, M., Harris, P.M., and Eberli, G.P., eds., Reservoir modeling:
1321 integration of outcrop and modern analogs: American Association of Petroleum Geologists, Memoir
1322 80, p. 45–66.
1323
1324 Yang, B., Dalrymple, R.W., Chun, S., Johnson, M.F., and Lee, H., 2008, Tidally modulated storm
1325 sedimentation on open-coast tidal flats, southwestern coast of Korea; distinguishing tidal flat from
1326 shoreface deposits, *in* Hampson, G.J., Steel, R.J., Burgess, P.M., and Dalrymple, R.W., eds., Recent
1327 advances in models of siliciclastic shallow-marine stratigraphy: SEPM, Special Publication 90, p. 161–
1328 176.
1329
1330 York, C.C., Painter, C.S., and Carrapa, B., 2011, Sedimentological characterization of the Sego
1331 Sandstone (NW Colorado, USA): a new scheme to recognize ancient flood-tidal-delta deposits and
1332 implications for reservoir potential: Journal of Sedimentary Research, v. 81, p. 401-419.
1333
1334 Yoshida, S., Willis, A., and Miall, A.D., 1996, Tectonic control of nested sequence architecture in the
1335 Castlegate Sandstone (Upper Cretaceous), Book Cliffs, Utah: Journal of Sedimentary Research, v. 66,
1336 p. 737–748.
1337
1338 Yoshida, S., Steel, R.J., and Dalrymple, R.W., 2007, Changes in depositional processes – an ingredient
1339 in a new generation of sequence-stratigraphic models: Journal of Sedimentary Research, v. 77, p. 447–
1340 460.
1341
1342 Young, R.G., 1955, Sedimentary facies and intertonguing in the Upper Cretaceous of the Book Cliffs,
1343 Utah-Colorado: Geological Society of America, Bulletin, v. 66, p. 177-202.
1344

Zapp, A.D., and Cobban, W.A., 1960, Some Late Cretaceous strand lines in northwestern Colorado and northeastern Utah: U.S. Geological Survey, Professional Paper 400-B, B246-B249.

TABLE AND FIGURE CAPTIONS

Figure 1

A) Paleogeography of central North America during the Campanian (after Roberts and Kirschbaum 1995), highlighting the location of the Book Cliffs outcrop belt. **B**) Map and **C**) cross-section along cliff line highlighting overall environments of deposition in the Sego Sandstone and surrounding lithostratigraphic units in the Book Cliffs (after Willis and Gabel 2001), the location of previous studies of the lower Sego Sandstone, and our study area (Fig. 2).

Figure 2

Map showing outcrop extent (gray line) and dataset collected for the lower Sego Sandstone within the study area. The locations of logged sections in Figure 6, correlation panels in Figure 8, and bedding diagram in Figure 9 are shown.

Figure 3

Photographs of wave-dominated deposits in the distal, lower Sego Sandstone: **A**) mudstone with intercalated wavy-bedded very fine-grained sandstone beds, within distal lower shoreface deposits (FA1); **B**) amalgamated, hummocky cross-stratified sandstones in proximal lower shoreface deposits (FA2); **C-E)** quasi-rhythmically interbedded hummocky cross-stratified and wave-rippled sandstones, recording possible tidal modulation in lower shoreface deposits (FA3), note lower micro-HCS bed is directly overlain by HCS without evidence of fair-weather mud deposition or bioturbation; and **F-H)** amalgamated low-angle cross-stratified sandstones (in lower 5 m of outcrop of Fig. 3F), interpreted as wave-reworked tidal bar deposits (FA4).

Figure 4

Photographs of mixed wave- and tide-influenced deposits in the distal, lower Sego Sandstone: **A**) ripple laminated and cross-bedded sandstone overlain by hummocky cross-stratified sandstone, recording deposition in a wave-influenced tidal bar (FA5), person for scale c. 1.8 m; **B-C**) transition from tidal bar (FA6) into wave-influenced tidal bar deposits (FA5); and **D**) measured section corresponding to Figure 4B.

Figure 5

Photographs of tide-dominated deposits in the distal, lower Sego Sandstone: **A**) coarsening-upward succession of heterolithic, cross-bedded sandstone interpreted as a tidal bar (FA6); **B**) mud-clast lag at the base of a tidal-bar succession (FA6), which passes gradationally upwards into **C**) wavy-bedded sandstones with intercalated dune-scale cross-sets (FA6), and then **D**) trough cross-bedded sandstone with mud drapes at the top of a tidal-bar succession (FA6); **E**) channelized sandstone, interpreted as an active tidal channel fill (FA7); **F**) herringbone cross-bedding with bimodal paleocurrents in the lower part of an active tidal channel fill (FA7), which passes gradationally upwards into **G**) wavy-bedded sandstones with mud-filled burrows of *Psilonichnus lutimuratus* (FA7); **H**) channelized mudstone, interpreted as an abandoned tidal channel fill (FA8); **I**) bioturbated mudsone in the lower part of an abandoned tidal channel fill (FA8), which passes gradationally upwards into **J**) an allochtonous coal (FA8).

Figure 6

Representative measured sections through the distal, lower Sego Sandstone illustrating facies-association successions and key stratigraphic surfaces in: **A)** a proximal setting, at Prairie Canyon (section 2 in Fig. 2); **B)** a medial setting, west of West Salt Creek (700 m northwest of section 6 in Fig. 2); and **C)** a distal setting, west of Dry Canyon (section 10 in Fig. 2). The locations of sections A and C are shown in Figures 2 and 8. Paleocurrent data for parts of each measured section are shown in rose diagrams.

Figure 7

Representative vertical sections synthesized from outcrop data through each of the facies associations in the distal, lower Sego Sandstone. Paleocurrent data collated for each facies association are shown in rose diagrams. Key to measured sections is the same as for Figure 6.

Figure 8

Correlation panels through the distal, lower Sego Sandstone, based on tracing of facies-association units and bounding surfaces along cliff faces between measured section. Panels are oriented sub-parallel to: **A)** regional depositional strike; and **B)** regional depositional dip (Fig. 2). The locations of the measured sections (Fig. 6), photograph (Fig. 4B) and bedding diagram (Fig. 9) illustrating detailed stratigraphic relationships are shown. Key to measured sections is the same as for Figure 6. Paleocurrent data for parts of each measured section are shown in rose diagrams. All facies boundaries are gradational unless indicated.

Figure 9

Bedding diagram showing detailed stratigraphic architecture and facies-association distribution in cliff-face exposure oriented sub-parallel to regional depositional dip, from the central part of the study area (Figs. 2, 8). Keys to measured sections and facies associations are the same as for Figures 6 and 8, respectively.

Figure 10

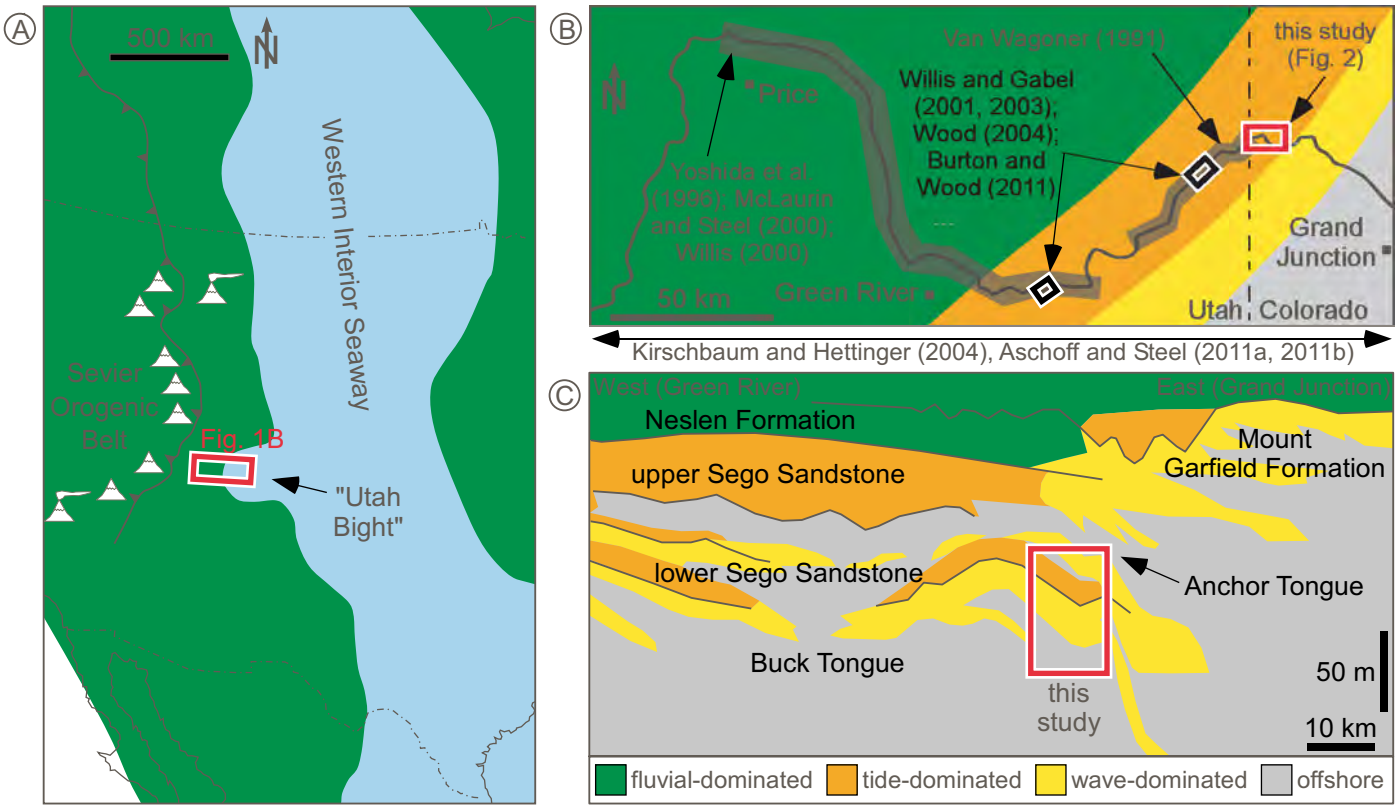
Facies-association distribution maps at maximum regression of four tide-dominated sandstone units (TS1-4) in the lower Sego Sandstone , each of which passes down depositional dip into coeval wave-dominated sandstone units (WS2, WS3, WS5, WS6) (Fig. 8): **A**) regional map of the "lower Sego Delta" (cf. Fig. 1B; after Willis and Gabel 2001); **B)** units TS1 and WS2; **C**) units TS2 and WS4; **D**) units TS3 and WS5; and **E**) units TS4 and WS6. The lower Sego Sandstone outcrop belt (Fig. 2) is shown to illustrate data distribution, and inferred distributions of facies associations away from the outcrop belt are shown in faded colors. **F**) Regional map of the modern Mekong Delta showing the location of **G)** line drawing of aerial view of a section of the mixed wave-and-tide-influenced delta front (based on GoogleEarth satellite image, Ta et al. 2005), at the same scale as lower Sego Sandstone facies-association distribution maps. The facies-association components and their spatial arrangement in this modern coastline are closely comparable to those interpreted in the ancient lower Sego Sandstone (Fig. 10B-E). Key to facies associations is the same as for Figure 8.

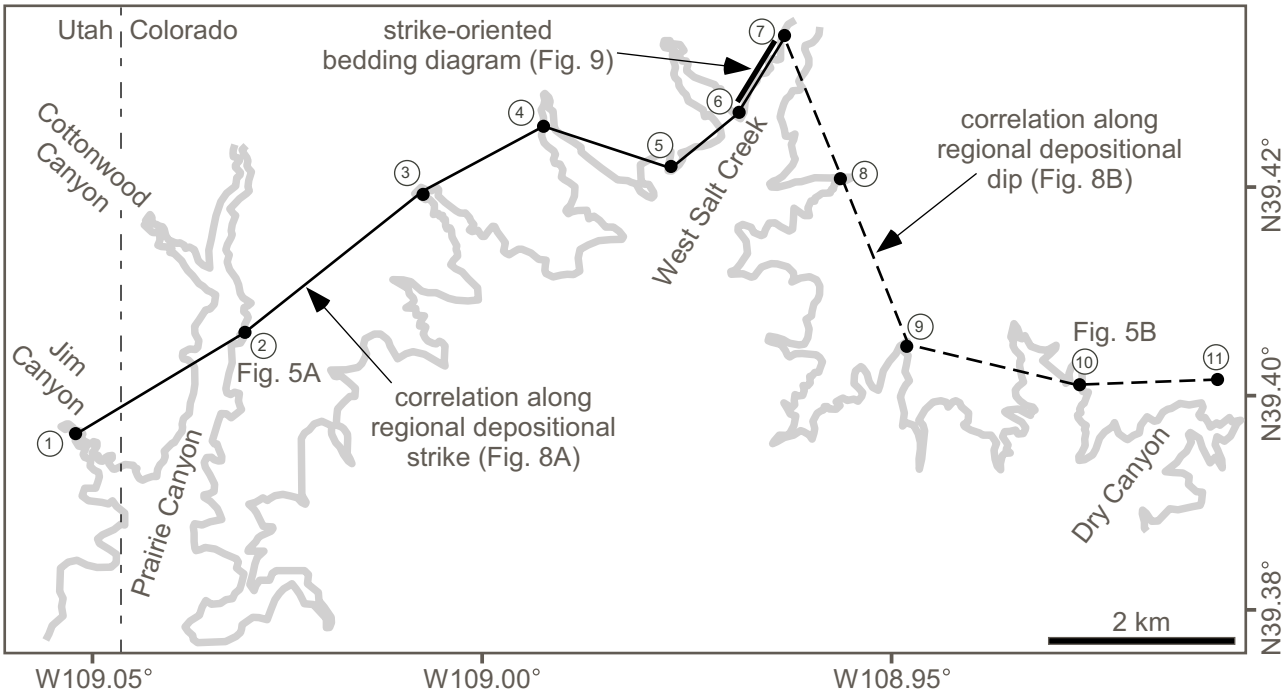
Figure 11

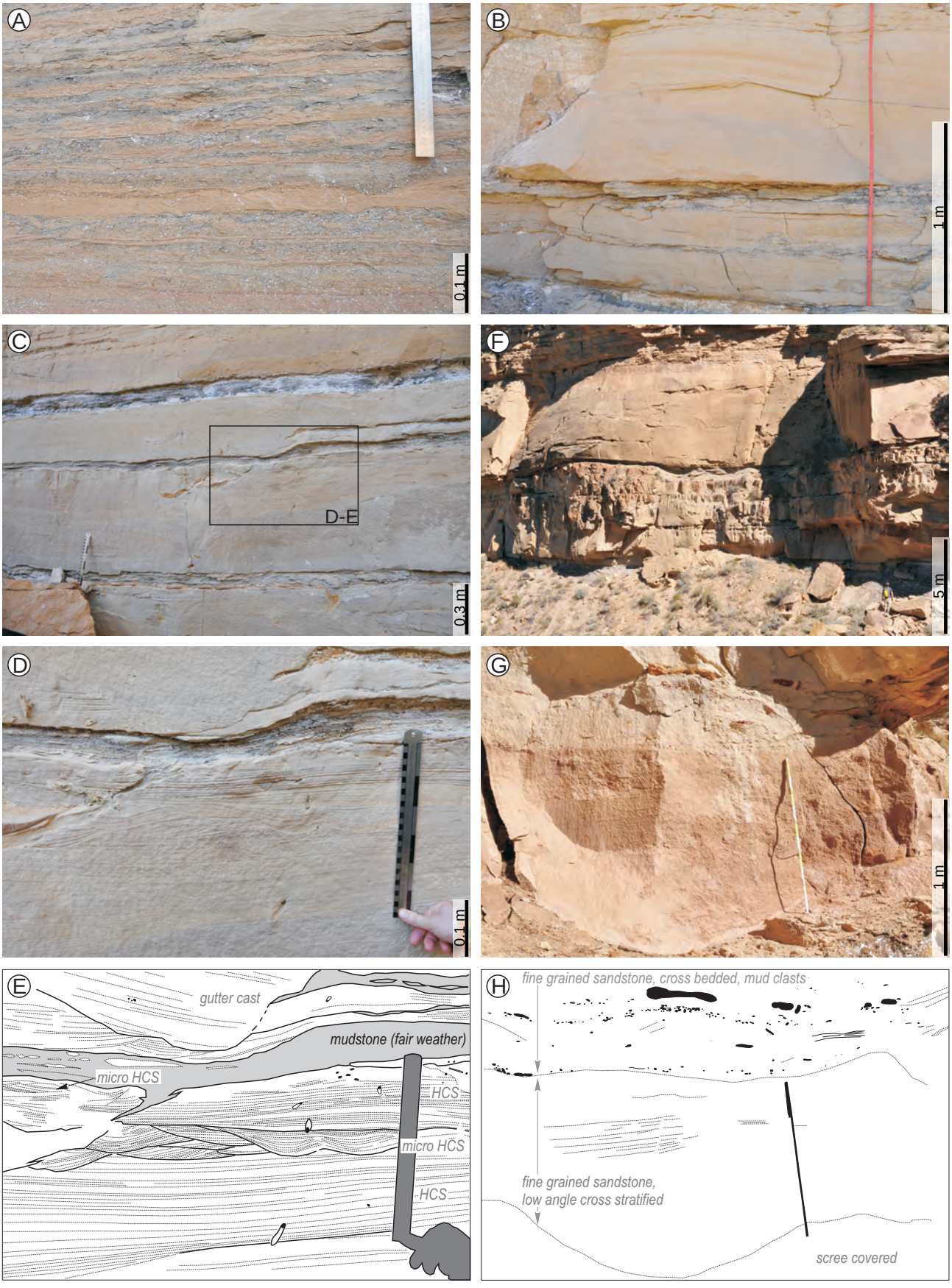
Model of tide-wave process interactions and resulting deposits along a dip section from tidal bars (proximal; FA6) to shoreface deposits (distal; FA3) (cf. Figs. 8, 10). In proximal locations (left), sand transport is dominated by tidal currents, but mud resuspension and offshore transport by waves results in clean tidal sandstones (FA6). In medial locations (center), increasing wave influence leads to reworking of dune crests by storm waves, causing sand to be transported offshore and redeposited as low-angle cross stratified and hummocky cross-stratified sandstone (FA4), and reworked dune tops are draped by hummocky cross-stratified, very fine-grained sandstone and laminated siltstone (FA5). In distal locations (right), sediment is principally transported by storm waves, but the influence of tides on water depths during storm events results in cyclic variations of bedform height (FA3). Storm-wave orbitals are not shown to scale.

Figure 12

Conceptual model of facies-association variability and distribution, and interaction of wave and tide processes in distal part of mixed, wave- and tide-influenced delta, based on the lower Sego Sandstone. The locations of representative measured sections (Fig. 7) are shown. Key to facies associations is the same as for Figure 8. Lateral migration of tidal channels and coeval tidal bars results in the development of low-relief erosional surfaces that juxtapose FA6 and FA7 above FA1 and FA2 in each regressive-transgressive tongue bounded by major flooding surfaces (FS100, FS200, FS300, and FS400) (Fig. 8).

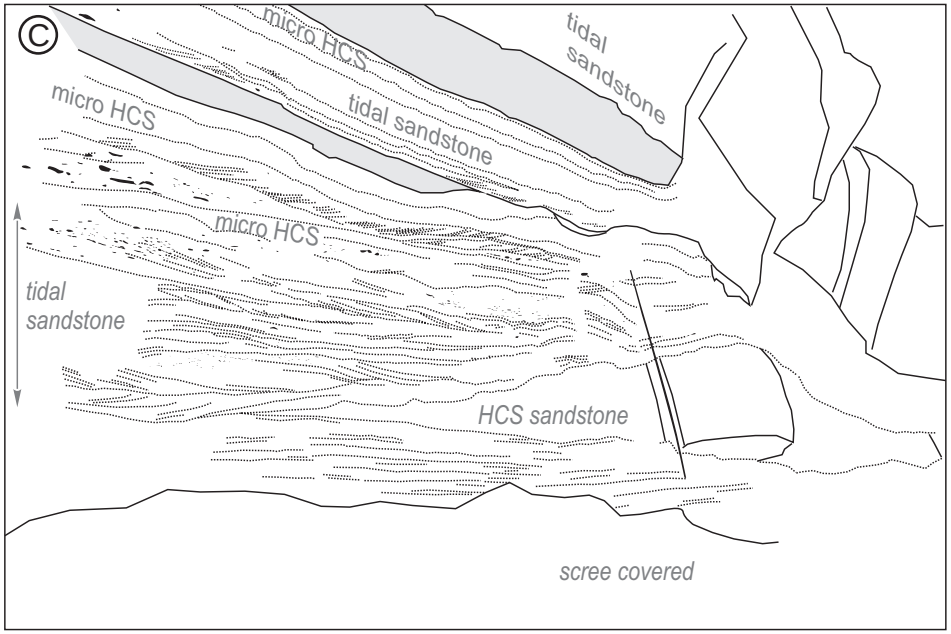

A
500 km
N
Western Interior Seaway
Sevier Orogenic Belt
Fig. 1B
"Utah Bight"
B
N
Price
Van Wagoner (1991)
this study (Fig. 2)
Willis and Gabel (2001, 2003); Wood (2004); Burton and Wood (2011)
Yoshida et al. (1996); McLaurin and Steel (2000); Willis (2000)
50 km
Green River
Grand Junction
Utah
Colorado
Kirschbaum and Hettinger (2004), Aschoff and Steel (2011a, 2011b)
C
West (Green River)
East (Grand Junction)
Neslen Formation
upper Sego Sandstone
Mount Garfield Formation
lower Sego Sandstone
Anchor Tongue
Buck Tongue
this study
50 m
10 km
fluvial-dominated
tide-dominated
wave-dominated
offshore

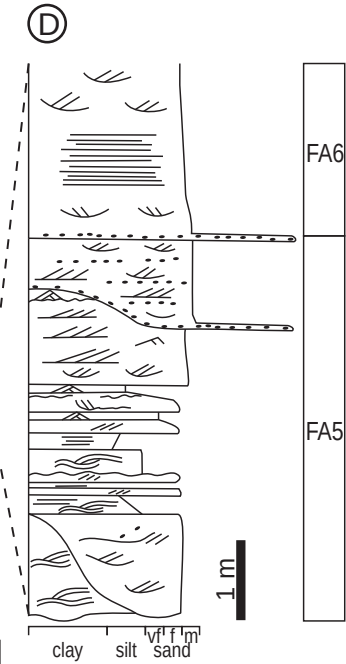

Utah
Colorado
strike-oriented
bedding diagram (Fig. 9)
Cottonwood
Canyon
Jim
Canyon
Prairie Canyon
West Salt Creek
Dry Canyon
correlation along
regional depositional
dip (Fig. 8B)
correlation along
regional depositional
strike (Fig. 8A)
Fig. 5A
Fig. 5B
1
2
3
4
5
6
7
8
9
10
11
2 km
W109.05°
W109.00°
W108.95°
N39.42°
N39.40°
N39.38°

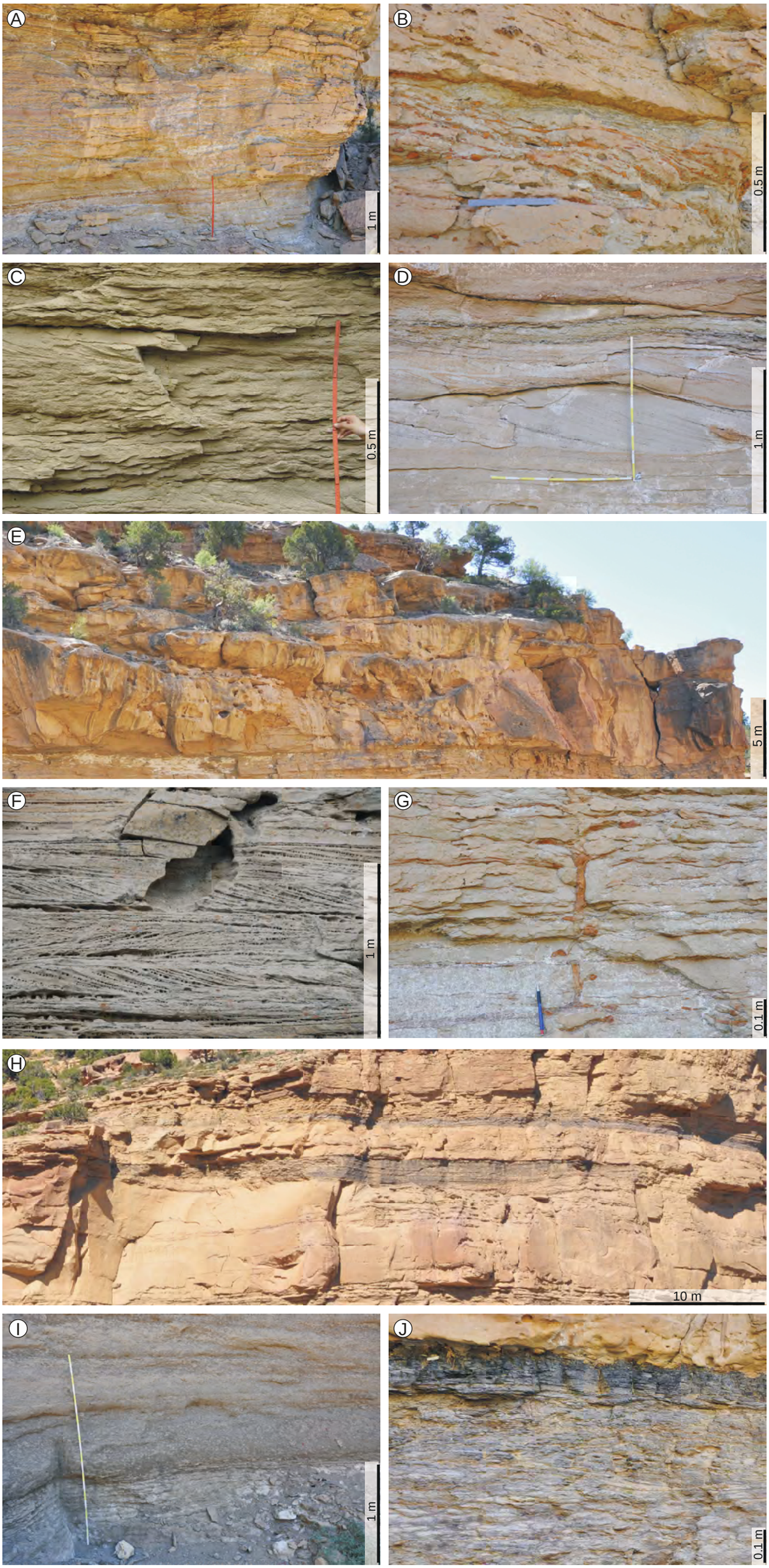

A
0.1 m
B
1 m
C
D-E
0.3 m
F
5 m
D
0.1 m
G
1 m
E
gutter cast
mudstone (fair weather)
micro HCS
HCS
micro HCS
HCS
H
fine grained sandstone, cross bedded, mud clasts
fine grained sandstone,
low angle cross stratified
scree covered

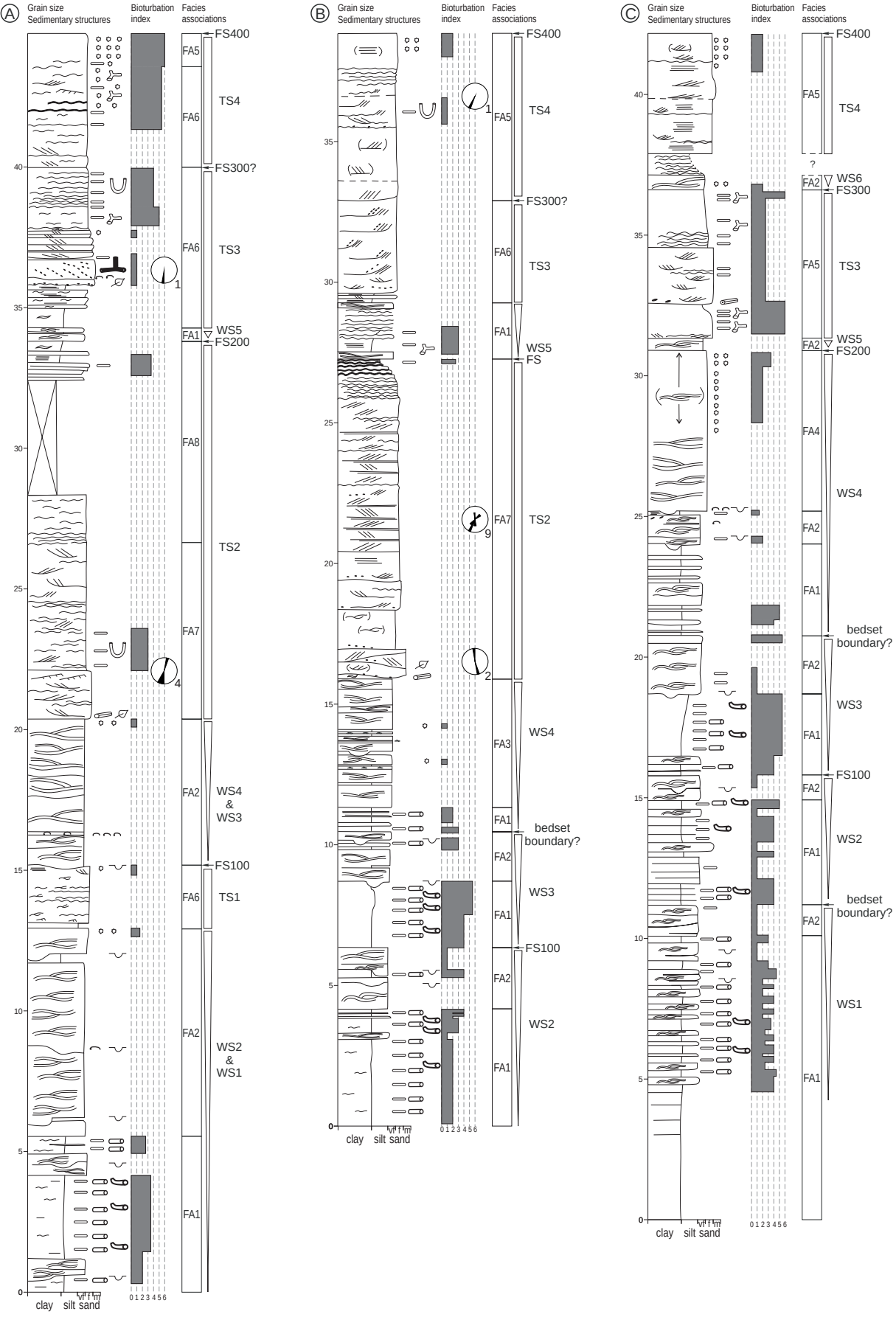

A

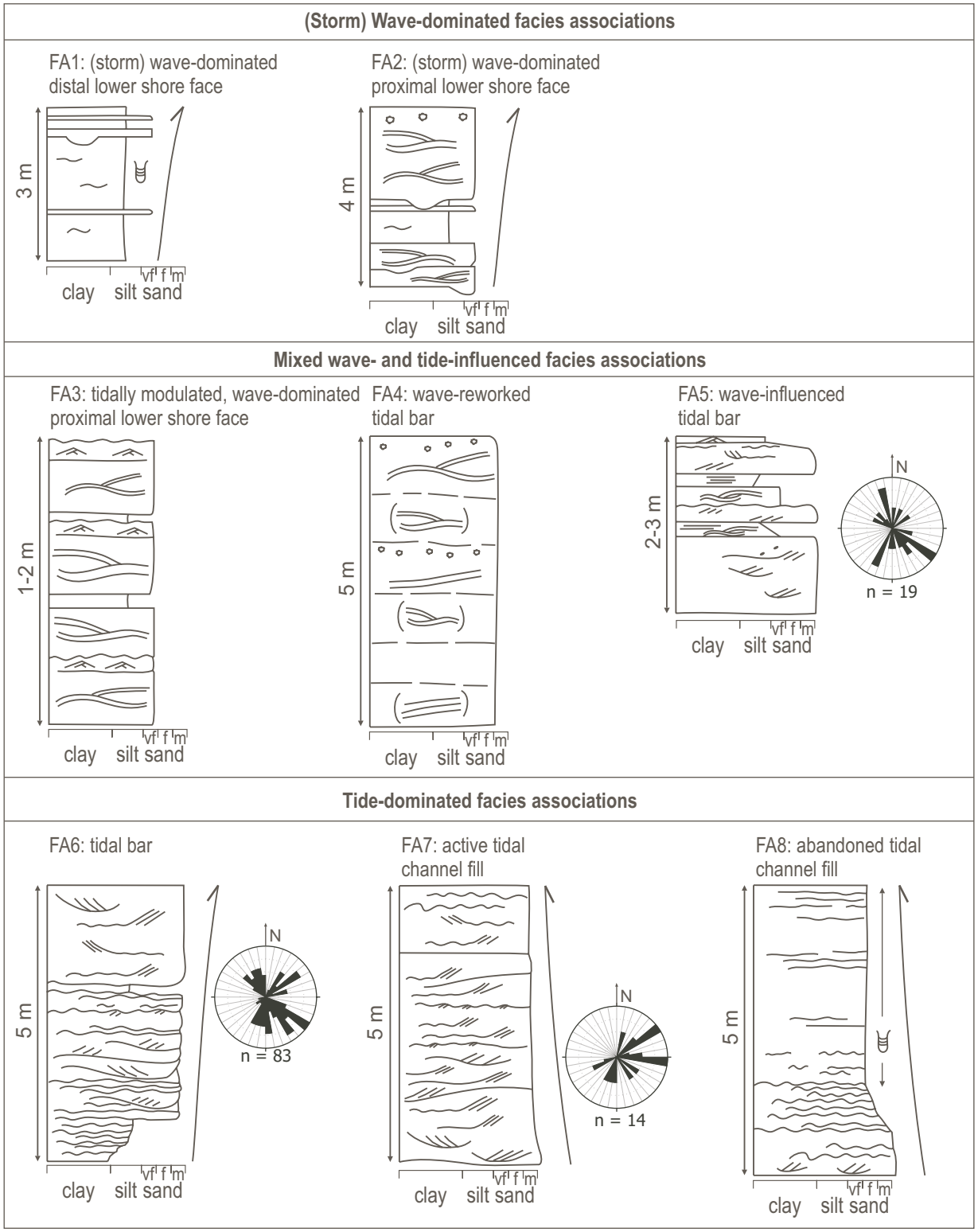

B

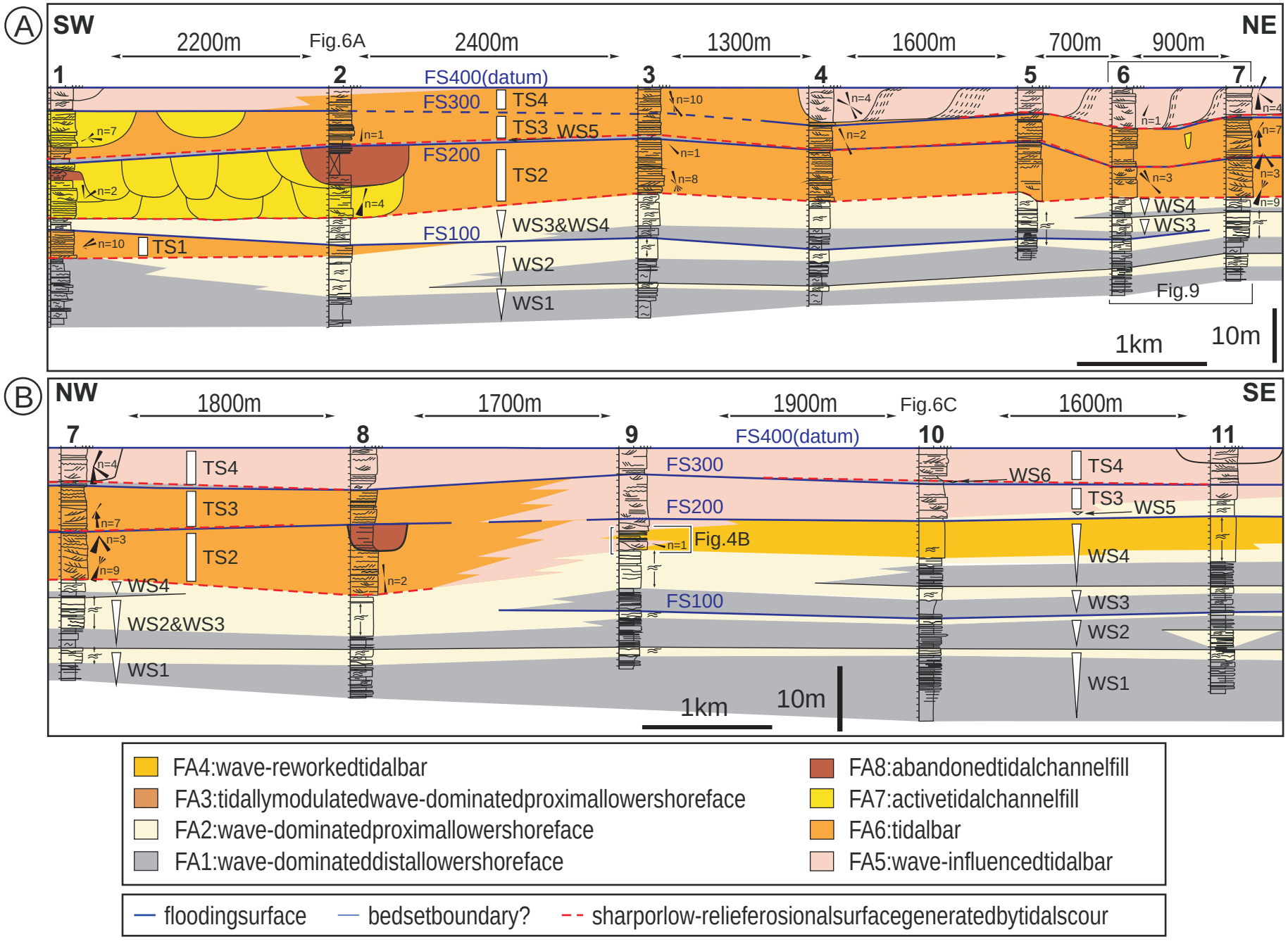

C
micro HCS
tidal sandstone
micro HCS
tidal sandstone
micro HCS
tidal sandstone
HCS sandstone
scree covered

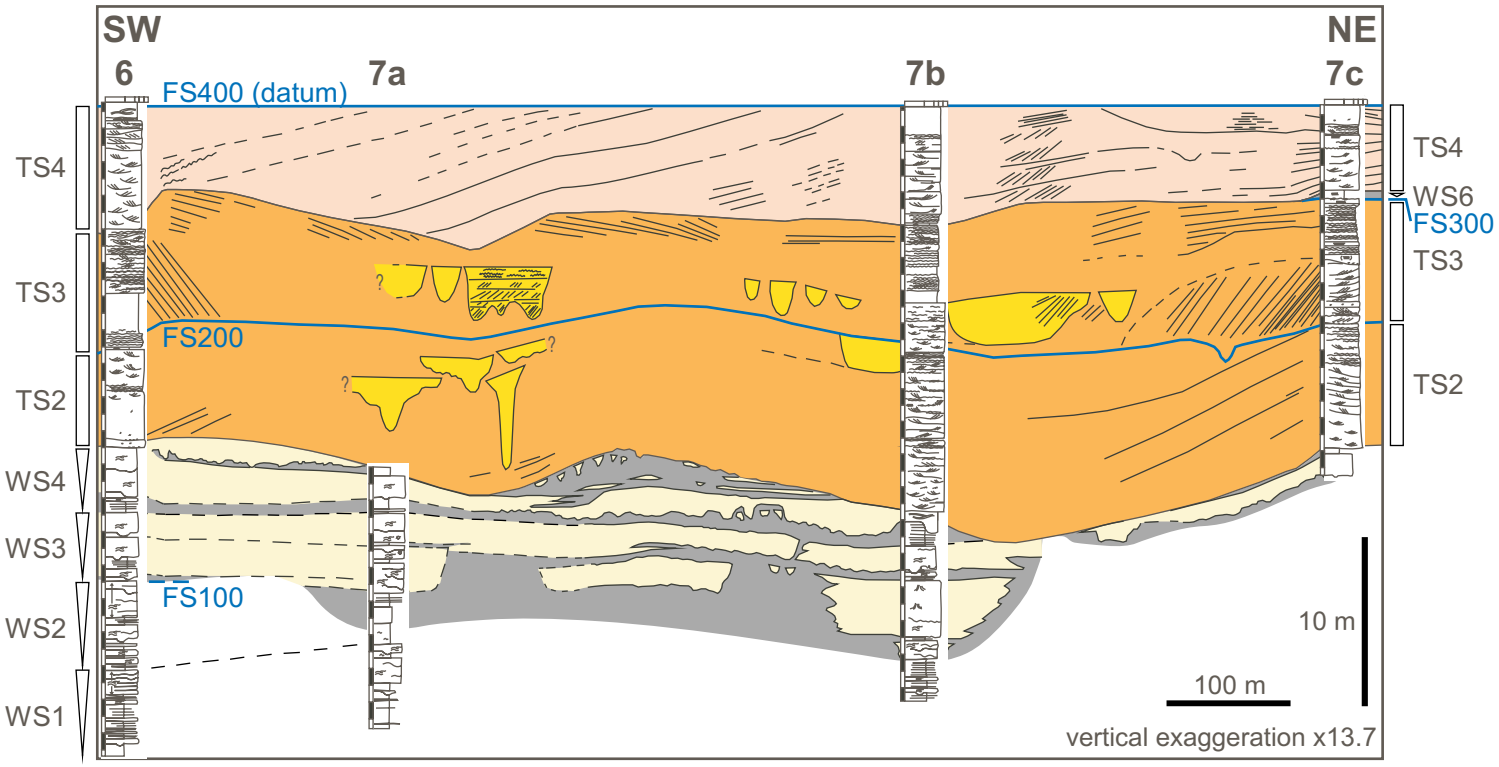

D
FA6
FA5
1 m
clay
silt
vf
f
m
sand

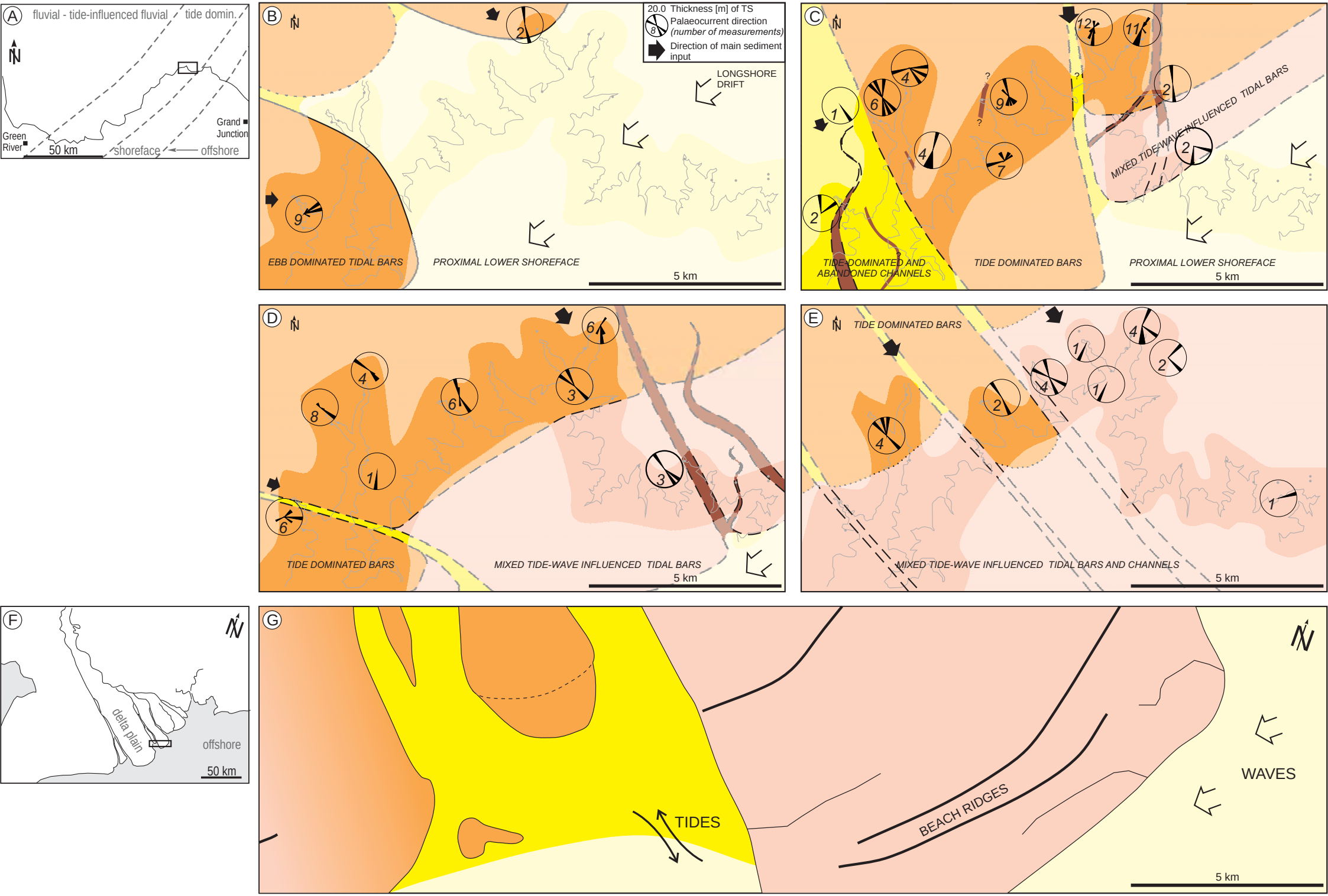

A
1 m
B
0.5 m
C
0.5 m
D
1 m
E
5 m
F
1 m
G
0.1 m
H
10 m
I
1 m
J
0.1 m

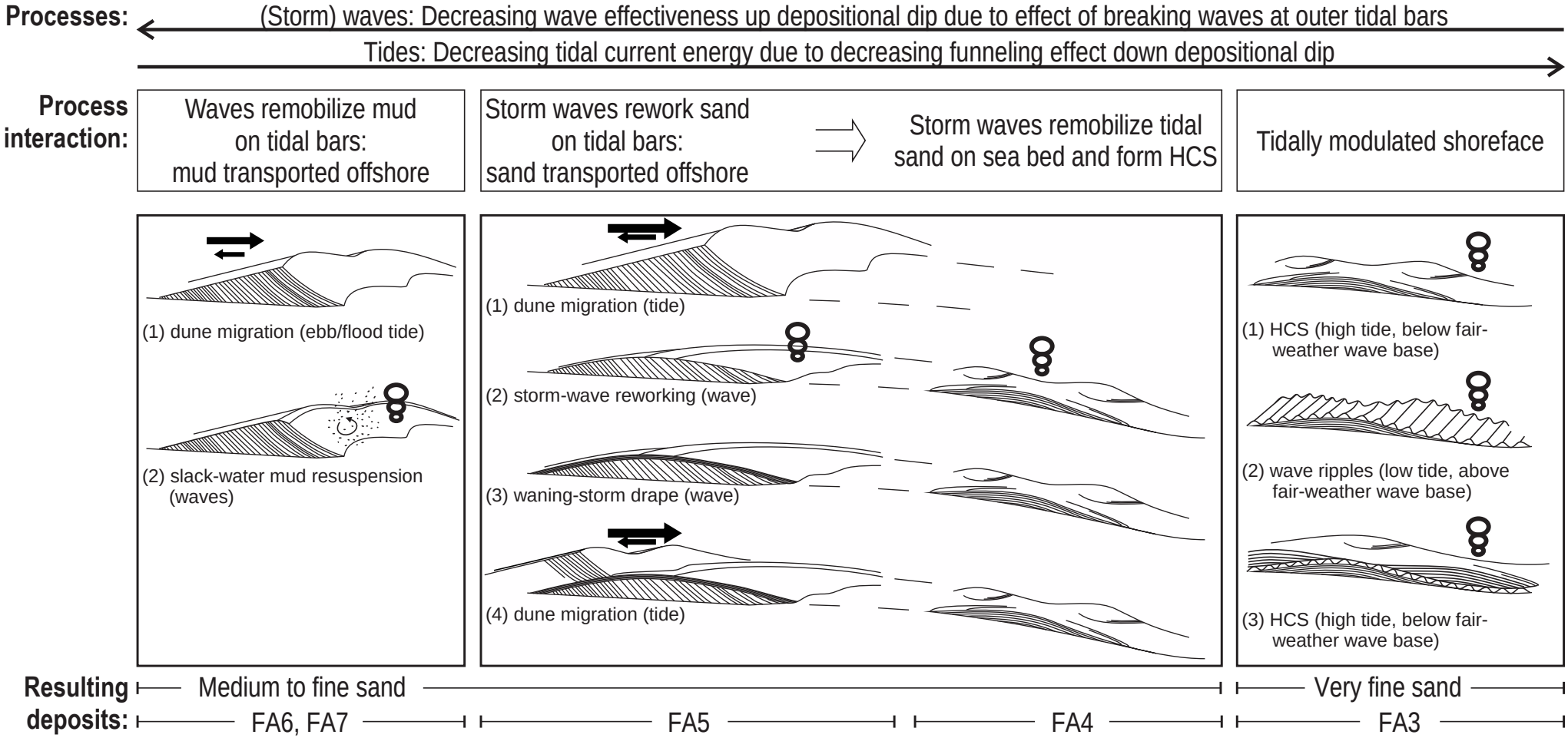

A
B
C
Grain size
Sedimentary structures
Bioturbation index
Facies associations
clay
silt
sand
FS400
TS4
FS300?
TS3
WS5
FS200
TS2
WS4 & WS3
FS100
TS1
WS2 & WS1
WS6
FS300
WS4
bedset boundary?
WS3
WS2
WS1
FS
Trough cross bedding
Planar cross bedding
Cross bedding with toesets
Mud clasts
Tabular bedding
Hummocky cross-stratification (HCS)
Gutter cast
Current ripple cross lamination
Wave ripple cross lamination
Shell debris
Plant fragments
Log (mostly with Teredolites)
Ophiomorpha nodosa
Thalassinoides
Arenicolites
Terebellina
Psilonichnus lutimeratus
Palaeophycos
Planolites

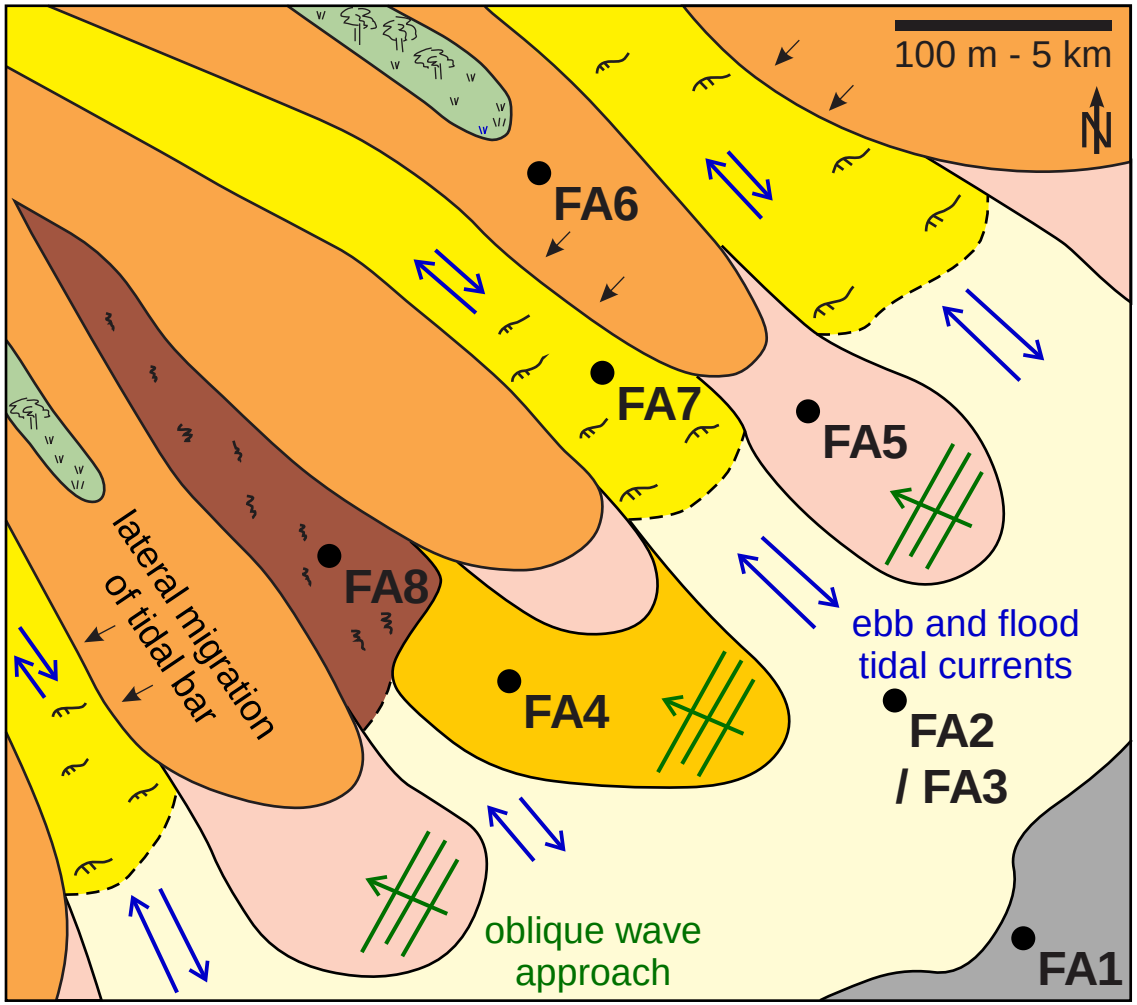

(Storm) Wave-dominated facies associations
FA1: (storm) wave-dominated distal lower shore face
3 m
clay
silt
sand
vf
f
m
FA2: (storm) wave-dominated proximal lower shore face
4 m
clay
silt
sand
vf
f
m
Mixed wave- and tide-influenced facies associations
FA3: tidally modulated, wave-dominated proximal lower shore face
1-2 m
clay
silt
sand
vf
f
m
FA4: wave-reworked tidal bar
5 m
clay
silt
sand
vf
f
m
FA5: wave-influenced tidal bar
2-3 m
clay
silt
sand
vf
f
m
N
n = 19
Tide-dominated facies associations
FA6: tidal bar
5 m
clay
silt
sand
vf
f
m
N
n = 83
FA7: active tidal channel fill
5 m
clay
silt
sand
vf
f
m
N
n = 14
FA8: abandoned tidal channel fill
5 m
clay
silt
sand
vf
f
m


A
SW
NE
2200m
Fig.6A
2400m
1300m
1600m
700m
900m
1
2
3
4
5
6
7
FS400(datum)
FS300
FS200
FS100
TS4
TS3
WS5
TS2
WS3&WS4
WS2
WS1
TS1
WS4
WS3
Fig.9
1km
10m
B
NW
SE
1800m
1700m
1900m
Fig.6C
1600m
7
8
9
10
11
FS400(datum)
FS300
FS200
FS100
TS4
TS3
TS2
WS4
WS2&WS3
WS1
WS6
WS5
Fig.4B
WS4
WS3
WS2
WS1
1km
10m
FA4:wave-reworkedtidalbar
FA3:tidallymodulatedwave-dominatedproximallowershoreface
FA2:wave-dominatedproximallowershoreface
FA1:wave-dominateddistallowershoreface
FA8:abandonedtidalchannelfill
FA7:activetidalchannelfill
FA6:tidalbar
FA5:wave-influencedtidalbar
floodingsurface
bedsetboundary?
sharporlow-relieferosionalsurfacegeneratedbytidalscour


SW
NE
6
7a
7b
7c
FS400 (datum)
FS200
FS100
FS300
TS4
TS3
TS2
WS6
WS4
WS3
WS2
WS1
10 m
100 m
vertical exaggeration x13.7


A
fluvial - tide-influenced fluvial
tide domin.
Green River
Grand Junction
50 km
shoreface
offshore
B
20.0 Thickness [m] of TS
Palaeocurrent direction
(number of measurements)
Direction of main sediment input
LONGSHORE DRIFT
EBB DOMINATED TIDAL BARS
PROXIMAL LOWER SHOREFACE
5 km
C
TIDE-DOMINATED AND ABANDONED CHANNELS
TIDE DOMINATED BARS
MIXED TIDE-WAVE INFLUENCED TIDAL BARS
PROXIMAL LOWER SHOREFACE
5 km
D
TIDE DOMINATED BARS
MIXED TIDE-WAVE INFLUENCED TIDAL BARS
5 km
E
TIDE DOMINATED BARS
MIXED TIDE-WAVE INFLUENCED TIDAL BARS AND CHANNELS
5 km
F
delta plain
offshore
50 km
G
TIDES
BEACH RIDGES
WAVES
5 km


Processes:
(Storm) waves: Decreasing wave effectiveness up depositional dip due to effect of breaking waves at outer tidal bars
Tides: Decreasing tidal current energy due to decreasing funneling effect down depositional dip
Process interaction:
Waves remobilize mud on tidal bars: mud transported offshore
Storm waves rework sand on tidal bars: sand transported offshore
Storm waves remobilize tidal sand on sea bed and form HCS
Tidally modulated shoreface
(1) dune migration (ebb/flood tide)
(2) slack-water mud resuspension (waves)
(1) dune migration (tide)
(2) storm-wave reworking (wave)
(3) waning-storm drape (wave)
(4) dune migration (tide)
(1) HCS (high tide, below fair-weather wave base)
(2) wave ripples (low tide, above fair-weather wave base)
(3) HCS (high tide, below fair-weather wave base)
Resulting deposits:
Medium to fine sand
Very fine sand
FA6, FA7
FA5
FA4
FA3


100 m - 5 km
N
FA6
FA7
FA5
FA8
FA4
FA2
/ FA3
FA1
lateral migration
of tidal bar
ebb and flood
tidal currents
oblique wave
approach